ELSEVIER

Earth-Science Reviews 55 (2001) 107–134

EARTH-SCIENCE REVIEWS

www.elsevier.com/locate/earscirev

Solifluction rates, processes and landforms: a global review

Norikazu Matsuoka *

Institute of Geoscience, University of Tsukuba, Tsukuba, Ibaraki 305-8571, Japan

Received 13 January 2000; accepted 14 March 2001

Abstract

Field data on the rates of solifluction and associated parameters are compiled from the literature, in an attempt to evaluate factors controlling the spatial variability in solifluction processes and landforms, with special attention on the climate–solifluction relationship. The analyzed data originate from 46 sites over a wide range of periglacial environments, from Antarctic nunataks to tropical high mountains. Solifluction, broadly defined as slow mass wasting resulting from freeze–thaw action in fine-textured soils, involves several components: needle ice creep and diurnal frost creep originating from diurnal freeze–thaw action; annual frost creep, gelifluction and plug-like flow originating from annual freeze–thaw action; and retrograde movement caused by soil cohesion. The depth and thickness of ice lenses and freeze–thaw frequency are the major controls on the spatial variation in solifluction processes. Near the warm margin of the solifluction-affected environment, diurnal freeze–thaw action induces shallow but relatively rapid movement of a superficial layer 5–10 cm thick on average, often creating the thin stone-banked lobes typically seen on tropical high mountains. In addition to diurnal movement, annual frost creep and gelifluction may occur on slopes with soil climates of seasonal frost to warm permafrost, dislocating a soil layer shallower than 60 cm at a rate of centimeters per year and eventually producing medium-size solifluction lobes. In High-Arctic cold permafrost regions, two-sided freezing can induce plug-like flow of a soil mass 60 cm or thicker. The correlation between process and landform suggests that the riser height of lobes is indicative of the maximum depth of movement and prevailing freeze–thaw type. Climate change may result in new different ground freezing conditions, thereby influencing the surface velocity and maximum depth of soil movement. Soil moisture and topography also control solifluction. High moisture availability in the seasonal freezing period enhances diurnal freeze–thaw action and subsequent seasonal frost heaving. The latter contributes to raising the moisture content of the thawed layer and promotes gelifluction during the thawing period. The slope angle defines the upper limit of the surface velocity of solifluction. A diagram correlating the potential frost creep with the actual surface velocity permits an inter-site comparison of the relative magnitude of solifluction components. Physically based modelling of periglacial slope evolution requires synthetic and more detailed field monitoring and laboratory simulations of solifluction processes.

Keywords: mass wasting; solifluction; freeze–thaw; permafrost; periglacial; climate change

1. Introduction

Freeze–thaw action induces downslope displacement of soils in cold, non-glacial environments, where vegetation is lacking or sparse (e.g., Wash-

* Fax: +81-298-51-9764.
E-mail address: matsuoka@atm.geo.tsukuba.ac.jp (N. Matsuoka).

0012-8252/01/$ - see front matter
PII: S0012-8252(01)00057-5

burn, 1979; Ballantyne and Harris, 1994; French, 1996). This process, broadly referred to as solifluction, operates slowly, in general at a rate of at most 1 m $year^{-1}$. In terms of geomorphic work, solifluction may influence the denudation of mountains much less than rapid processes and geochemical transfers (e.g., Rapp, 1960; Smith, 1992). However, its widespread distribution on mountain slopes means that solifluction contributes greatly to the evolution of mountain landscapes. Moreover, landforms and subsurface structures resulting from solifluction are strongly dependent on climatic conditions. This implies that solifluction features can be used as an indicator of the climate that has affected the slope in the past (e.g., Benedict, 1976; Bertran et al., 1995).

Rates and processes of solifluction depend, in collective terms, on climate, hydrology, geology and topography. Prediction of landscape evolution in periglacial mountains requires quantitative relationships between the rate of solifluction and these variables (Lewkowicz, 1988; Kirkby, 1995). For this purpose, field measurements have been undertaken in a variety of geographical situations ranging from polar hillslopes (e.g., Washburn, 1967) to tropical high mountains (e.g., Francou and Bertran, 1997) and, as a result, a large number of data-nets on solifluction rates and associated parameters have been obtained.

Recent progress in field methodology has allowed the evaluation of the timing and environmental conditions at which soil movement occurs (e.g., Matsuoka et al., 1997; Lewkowicz and Clarke, 1998). Laboratory simulations have also added knowledge of the mechanisms involved in solifluction processes (Harris et al., 1993, 1997). These advances will enable us to link solifluction rates with their controlling factors, eventually permitting the construction of a physically based predictive model of solifluction.

This paper compiles the extant field data from a wide range of periglacial environments and presents quantitative relationships between the rates and landforms of solifluction and a variety of parameters. Analysis of these relationships permits understanding of factors affecting the spatial variability in solifluction processes and landforms. A particular focus is on climate–solifluction linkages. Finally, the possible effect of climatic change on solifluction is discussed.

2. Terminology

The term ‘solifluction’ has not yet been defined unequivocally. The original meaning was the slow downslope movement of saturated soil occurring in cold regions (Andersson, 1906). Later studies have revealed that slow mass movements in cold regions include several processes and do not necessarily require saturation. In modern usage, solifluction represents collectively slow mass wasting associated with freeze–thaw action (Ballantyne and Harris, 1994; French, 1996), and the saturated soil movement associated with ground thawing is designated as gelifluction (Washburn, 1979). This paper follows the modern broad terminology. In other words, solifluction precludes rapid slope failures that reflect slide or flow over a shear plane, such as active-layer detachment slides and skinflows (e.g., Lewkowicz, 1988; Ballantyne and Harris, 1994), although only a slight difference in moisture or slope inclination may define the boundary between the slow and rapid movements. In the light of soil properties, solifluction is favored by sandy to silty soils having low liquid limits and plasticity indices (Harris, 1989).

Solifluction is classified into needle ice creep, frost creep, gelifluction and plug-like flow, using the criteria of the locus of particles and the vertical extent of movement that reflects the depth at which ice lenses develop during frost heaving (Fig. 1). Frost creep is the downslope movement of soil particles originating from frost heaving normal to the slope followed by nearly vertical thaw consolidation (Washburn, 1979). Cohesion between soil particles may induce retrograde movement on thawing. Frost creep can be subdivided into *diurnal frost creep* and *annual frost creep* in accordance with the period for the completion of a freeze–thaw cycle. The difference in frost duration affects the depth of ice lenses developing during frost heaving, and thus controls the depth of movement (Fig. 1B and C). Accordingly, diurnal frost creep mainly dislocates the uppermost few centimeters of soil (e.g., Matsuoka, 1998a), while annual frost creep usually occurs at a depth of a few decimeters (e.g., Smith, 1988).

Needle ice creep, a special kind of diurnal frost creep, occurs when surface debris (one to few grains thick) is lifted by ice needles and falls on thawing (Fig. 1A). The growth of ice needles reflects noctur-

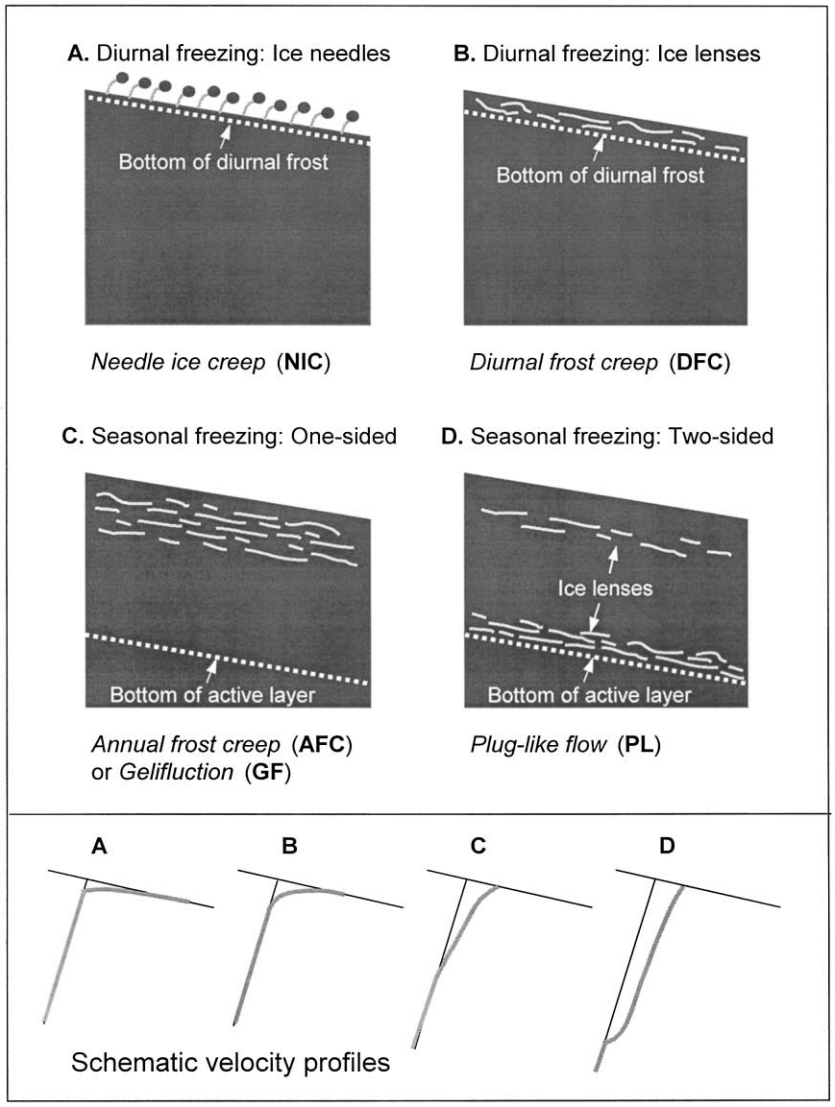

Fig. 1. Types of frost heave and solifluction.

nal cooling to just below 0°C, during which the frost plane stays within the uppermost centimeter of soil. Such a thermal condition mainly occurs in early winter when the subsurface soil is still warm enough to prevent nocturnal frost penetration (e.g., Matsuoka, 1994). The mechanical weakness of the ice needles often results in toppling or rotational downslope movement of the grains (Higashi and Corte, 1971; Mackay and Mathews, 1974). As a result, the repetition of diurnal freeze–thaw cycles leads to superficial but relatively rapid movement.

Gelifluction is mainly associated with seasonal thawing (Fig. 1C), when a plastic soil layer originates from thaw consolidation of the seasonally frozen ground and/or inflow of additional water from snowmelt or rainfall. The raised moisture content may induce soil deformation at a pre-failure stress level (Harris et al., 1997), resulting in slow

downslope displacement of the soil mass. The identification of the gelifluction component in the total soil movement is often difficult, since it may be confused with annual frost creep and retrograde components.

The final type of solifluction is *plug-like flow*, which takes place exclusively on slopes underlain by cold permafrost (e.g., Mackay, 1981). The ground in non-permafrost and warm permafrost areas mostly undergoes one-sided (downward) freezing. No matter how deep the frost plane penetrates, desiccation associated with ice segregation in the upper soil hinders ice lens growth at depth. In contrast, two-sided (both downward and upward) freezing can occur in the presence of cold permafrost, because a large thermal gradient permits the upward frost penetration from the top of permafrost (Lewkowicz, 1988). The upward freezing may produce numerous ice lenses near the base of the frozen active layer, which on thawing induce movement of the whole active layer as a plug (Fig. 1D). Plug-like flow may involve both 'deep' gelifluction and rapid sliding (e.g., Williams and Smith, 1989; Lewkowicz, 1992a). The boundary between warm and cold permafrost that delimits the occurrence of two-sided freezing is so far unclear, but analysis of soil movements will help define this boundary.

3. Data collection

Data for analysis are compiled from the literature, mostly written in English or Japanese. The compilation basically excluded data derived from screes and slopes subjected mainly to rapid failures. Language barriers may also have induced omission of some useful data. In total, data from 46 sites were analyzed. Available data are biased to the northern hemisphere, in particular, from the Arctic regions to mid-latitude high mountains, while only a few data are available from the Antarctic. The following parameters and information are listed in Tables 1 and 2. Where a significant difference in movement occurs between landform types within a study site (e.g., Benedict, 1970; Åkerman, 1996), data are summarized for each landform type.

3.1. Landforms and topographic parameters

Types and dimensions of characteristic surface features developed at the measurement site are relevant information, because they reflect rates and processes of solifluction. Landforms are grouped into lobes, terraces (or steps), stripes and hummocks; some examples are shown in Fig. 2. A synonym of lobes is sheets. Whereas lobes are more common on alpine slopes where surface conditions (vegetation, material and topography) are variable, sheets are associated with homogeneous surface conditions which dominate on polar slopes (e.g., Harris, 1981). Hereafter, lobes and sheets are collectively called lobes and subdivided in terms of the presence of vegetation into turf-banked and stone-banked lobes. Similarly, the terrace group is classified into turf-banked and stone-banked terraces. The definition of these features basically follows Benedict (1970), although there is no sharp boundary between lobes and terraces (Harris, 1981). The turf-banked forms include both those having complete vegetation cover and those having vegetation only on the riser. Grazing steps, a terracette-like form produced by the activity of cattle and possibly modified by freeze–thaw processes, develop at some sites. The stripe group consists of sorted and non-sorted stripes. Stripes and hummocks are sometimes superimposed on a larger lobe or sheet, producing a complex form. Sites showing no specific form are described as smooth slopes.

Fig. 2. Solifluction features and movement. The annual velocity profiles were based on the cumulative subsurface movement for 2–4 years, measured with flexible tubes or strain probes: a profile represents a tube. (A) Small sorted stripes developed on the top of a limestone slope (Upper Engadin, Swiss Alps; 2810 m ASL). (B) Stone-banked lobes developed near the base of a limestone slope (Upper Engadin, Swiss Alps; 2690 m ASL). (C) A turf-banked sheet composed of muddy sediments derived from the schist bedrock, overriding sandy marine sediments (Kapp Linné, Svalbard; 30 m ASL). (D) Large non-sorted stripes developed on muddy sediments derived from the shale bedrock (Adventdalen, Svalbard; 270 m ASL).

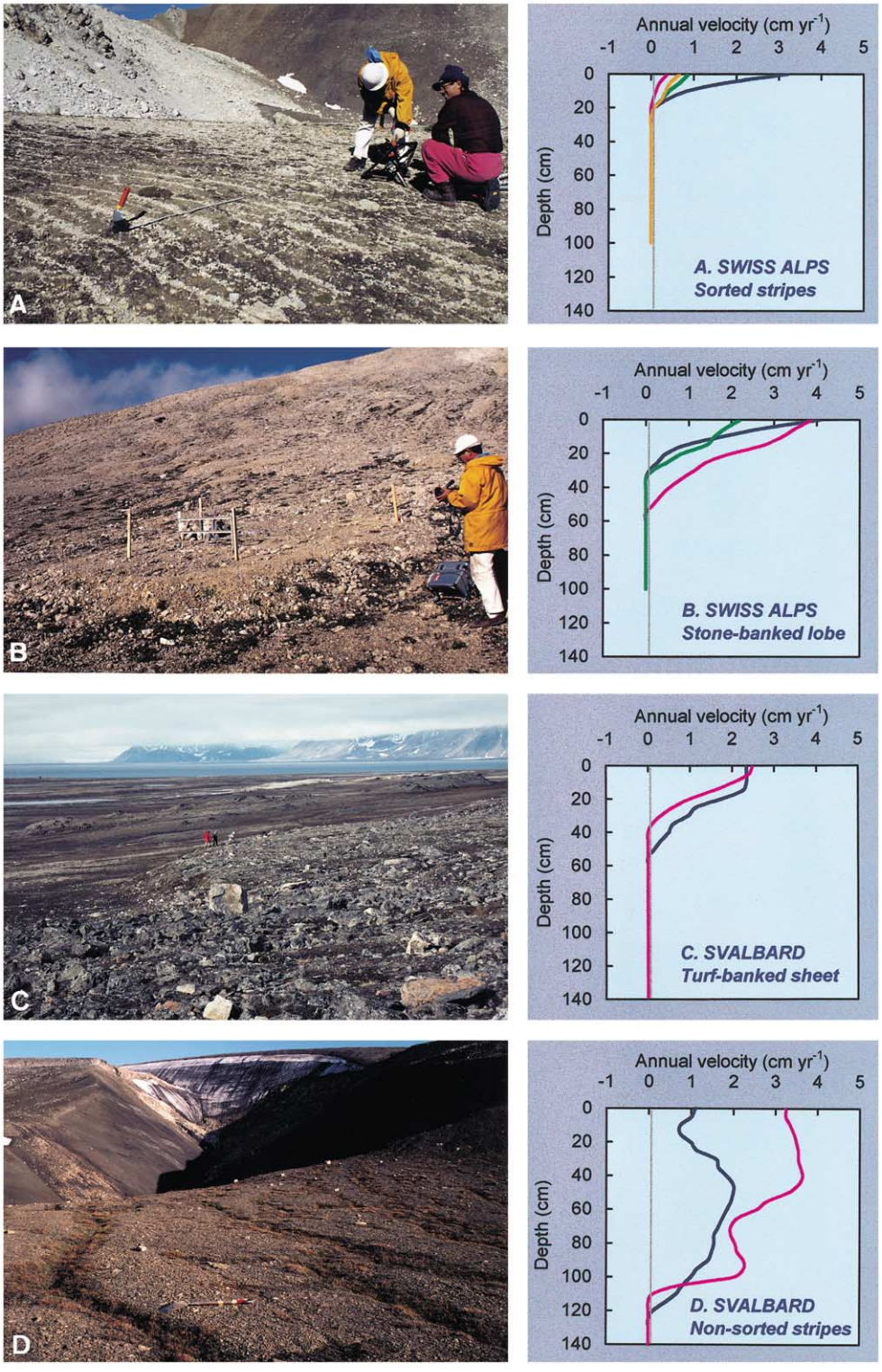
A
Annual velocity (cm yr-1)
-1 0 1 2 3 4 5
Depth (cm)
0 20 40 60 80 100 120 140
A. SWISS ALPS
Sorted stripes
B
Annual velocity (cm yr-1)
-1 0 1 2 3 4 5
Depth (cm)
0 20 40 60 80 100 120 140
B. SWISS ALPS
Stone-banked lobe
C
Annual velocity (cm yr-1)
-1 0 1 2 3 4 5
Depth (cm)
0 20 40 60 80 100 120 140
C. SVALBARD
Turf-banked sheet
D
Annual velocity (cm yr-1)
-1 0 1 2 3 4 5
Depth (cm)
0 20 40 60 80 100 120 140
D. SVALBARD
Non-sorted stripes

Table 1
Solifluction data in polar to subpolar regions

Location	MAAT (°C)	Frost type[a]	Frost (thaw) penetration[b] (cm)	Slope gradient (°)	Monitoring period (year)	Maximum heave (cm)
Ellesmere Is., Can. Arctic	−19	CPF	60T	5–9	5	nd
Sør Rondane, Antarctica	−18.4	CPF (DT)	15T	11–20	4	0.2
Melville Is., Can. Arctic	−16.5	CPF	31T	4.5	2–3	18.5
Cornwallis Is. Can. Arctic	−16.5	CPF	70T	7	8	nd
Banks Is., Can. Arctic	−14.5	CPF	90T	2–8	11	nd
Garry Is., Can. Arctic	−11	CPF	60T	3–7	13	14.4
Garry Is., Can. Arctic	−11	CPF	60T	3–7	11–12	nd
NE Greenland	−9.7	CPF	100–200T	10–14	5	nd
Svalbard	~ −8	CPF	> 100T	6–31	6	3.0
Svalbard	~ −7	CPF	110T	7–15	2	5.0
SW Yukon, Canada	~ −7	CPF	> 100T	14–18	16–21	nd
Schefferville, Canada	−5	WPF	150–300T	8	3	nd
Svalbard	~ −5	CPF	80T	10	2	8.8
Svalbard	~ −5	CPF	100T	10	nd	nd
Svalbard	−4.9	CPF	130T	20	2	nd
Svalbard	−4.9	CPF	50T	2–10	23	nd
Svalbard	−4.9	CPF	40T	4–12	23	nd
Svalbard	−4.9	CPF	65T	2–8	23	nd
Svalbard	−4.9	CPF	50T	6–20	23	nd
Svalbard	−4.9	CPF	45T	6–20	23	nd
Svalbard	−4.9	CPF	50T	8–25	23	nd
Svalbard	−4.9	CPF	80T	28–36	23	nd
Svalbard	−4.9	CPF	65T	2–10	23	nd
Kebnekaise, N Sweden	−4	WPF	> 80T	7–25	8	1
Abisko Mts., N Sweden	−4	WPF	nd	10–25	2–3	nd
Abisko Mts., N Sweden	−4	WPF	nd	5–20	1–3	nd
Abisko Mts., N Sweden	−4	WPF	nd	20	4	nd
Abisko Mts., N Sweden	~ −3	WPF	nd	16	17	> 2
Okistindan, N Norway	~ 0	SF	> 200F	5–17	1	2–6
South Georgia, Subantarctic	1.3	SF	> 200F	21	1	9.5
Macquarie Is., Subantarctic	~ 2	SF	nd	10–15	5	nd
Iceland	~ 4	SF	nd	7–10	2	nd

Throughout the table, the asterisk indicates mean values and 'nd' indicates no data or not mentioned.

[a] CPF, Cold permafrost; WPF, warm permafrost; SF, seasonal frost; DF, diurnal frost; DT, diurnal thaw.

[b] T, Maximum thaw depth; F, maximum frost depth.

[c] Non-electric methods: MS, marked stones; TR, tilting rods; PG, pegs (wood, plastic); CM, columns (wood, plastic, etc.); AF, aluminum foil strips; PT, plastic tubes. Electoric methods: IC, inclinometers; SP, strain probes; SM, solifluction meter.

[d] NIC, Needle ice creep; DFC, diurnal frost creep; AFC, annual frost creep; GF, gelifluction; PL, plug-like flow; ALG, active layer glide; MF, mudflow; TC, talus creep.

[e] SSP, Sorted stripes; NSP, non-sorted stripes; SBL, stone-banked lobes; TBL, turf-banked lobes; SBT, stone-banked terraces; TBT, turf-banked terraces; HK, hummocks; GS, grazing steps; SS, smooth slope; TL, talus slope.

[f] S, Stripe spacing; H, riser height.

Surface velocity (cm year^{-1})	Depth of movement (cm)	Methods of measurement[c]	Major processes[d]	Landforms[e] (dimensions in cm)[f]	Reference
1.7–3.1	60	SM, CM, PT	PL, AFC	SS	Lewkowicz and Clarke (1998)
1.0*	12	SP	DFC	SS	Matsuoka and Moriwaki (1992)
1.6	> 65	MS, AF, IC	AFC, GF, PFC	NSP	Bennett and French (1991)
3.0*	nd	PG	AFC, GF	SSP	Washburn (1999)
0.6*	nd	MS, AF	MF, AFC, GF, PL	NSP (150–200S), HK	Egginton and French (1985)
0.7	60	PT	PL	HK	Mackay (1981)
0.5	60	PT	PL	TBL (50H), HK	Mackay (1981)
0.9–3.7	nd	PG	AFC, GF (wet site)	SBL, TBL (< 300H), TBT	Washburn (1967)
3.0*	51–90	MS, PT	GF > AFC > DFC	SBL, NSP	Sawaguchi (1995)
2.2*	110	PT	GF, PL	NSP (250S)	Matsuoka and Hirakawa (2000)
1.3*	52*	PT, SP, MS	GF, ALG	TBL (100–200H)	Price (1973, 1991)
9	65	PT(IC)	AFC, MF	SBL, TBL	Williams (1966)
3–4	nd	PG	GF	SBL	Jahn (1985)
5.1*	nd	PG	GF	TBL, TBT (40H)	Repelewska-Pękalowa and Pękala (1993)
2.5*	48	PT	GF	TBL (50H)	Matsuoka and Hirakawa (2000)
4.4*	45	MS, AF, CM	nd	SBL (65H)	Åkerman (1996)
3.5*	30	MS, AF, CM	nd	SBL (35H)	Åkerman (1996)
2.3*	25	AF, CM	nd	TBT (25H)	Åkerman (1996)
0.9*	30	MS, AF, CM	nd	SBT (30H)	Åkerman (1996)
2.1*	15	PG, AF, CM	nd	NSP	Åkerman (1996)
1.5*	35	MS, CM	nd	SSP	Åkerman (1996)
6.8*	nd	MS	TC	TL	Åkerman (1996)
4.1*	35	MS, AF, CM	nd	SS	Åkerman (1996)
1.9*	39*	CM	AFC, GF	TBL	Jahn (1991)
0.8*	nd	MS	nd	SSP	Rudberg (1962)
2.4*	60	MS, CM	nd	TBL	Rudberg (1962)
5.2*	nd	PG	GF	TBL (50H)	Nyberg (1993)
3.1*	nd	MS, PG	nd	TBL (70H)	Rapp and Åkerman (1993)
2.1*	30*	PG, PT	AFC, GF	TBL (50–150H)	Harris (1972)
47*	25	MS, PG	AFC, NIC	SSP	Smith (1960)
38–138	nd	MS	nd	TBT (100–200H)	Selkirk (1998)
0.9*	20	CM	GF	TBT (39H)	Douglas and Harrison (1996)

A number of the references describe the dimensions of these forms, of which two parameters, the height of lobes (or terraces) and the spacing of stripes, are listed in Tables 1 and 2. If a dimension relates to a process parameter, the dimension may, in turn, indicate the nature of movement. Another important topographic parameter is the inclination of the studied slope θ, which ranges from 2° to 41°, with the mode between 10° and 20°.

3.2. Environmental parameters

The environmental parameters examined are the mean annual air temperature (MAAT), frost type and

Table 2
Solifluction data in mid-latitude to tropical mountains

Location	MAAT (°C)	Frost type[a]	Frost (thaw) penetration[b] (cm)	Slope gradient (°)	Monitoring period (year)
N Tibetan Plateau	−6	WPF	> 200T	15–25	5
W Tianshan, Kazakhstan	~ −5	WPF	nd	5–25	20
Daisetsu Mts., N Japan	−5	WPF	nd	12–27	8
Colorado Front Range, USA	~ −3	WPF	nd	13	5
Colorado Front Range, USA	~ −3	WPF	nd	12.5	3
Colorado Front Range, USA	~ −3	WPF	> 120T?	6–7	4
Colorado Front Range, USA	~ −3	WPF	nd	11–12	3
Colorado Front Range, USA	~ −3	WPF	nd	16–18	2
Colorado Front Range, USA	~ −3	WPF	> 150T?	14	6
Colorado Front Range, USA	~ −3	WPF	nd	13.5	6
Colorado Front Range, USA	~ −3	WPF	nd	12	3
Colorado Front Range, USA	~ −3	WPF	nd	5–7	6
E Tianshan, China	~ −3	WPF	nd	21–29	3
E Tianshan, China	−3	WPF	160T	20	2
Swiss Alps	−3	WPF/SF	200F	7	4
Swiss Alps	−3	WPF/SF	200F	12	4
Canadian Rockies	−2	SF	> 75F	21	9–10
Hohe Tauern, Austria	−2	SF	80F	10–20	2
S Japanese Alps	−2	SF	> 150F	14–30	3
Coast Mts., Canada	~ −2	SF	5F	10–15	10
Olympic Mts., USA	~ −1	SF	nd	12–24	8
Bolivian Andes	~ −1	DF	20F	19–28	3–5
N Japanese Alps	~ −1	SF	> 50F	11–30	2
Swiss Alps	−0.8	SF	> 100F	ca. 25	4
French Alps	~ 0	SF	nd	2–34	16–32
Central Otago, New Zealand	~ 0	SF	> 20F	7–14	20
Venezuelan Andes	~ 1	DF	6–9F	18–25	4
Venezuelan Andes	~ 1	DF	7–13.5F	19–25	4
Lake District, N England	~ 3	SF	nd	15	0.7
Kitakami Mts., N Japan	4.2	SF	90F	10	2
Nikko, central Japan	6.6	SF	15F	28–41	1–2
Nagano, central Japan	6.7	SF	28F	22	0.5
Nagano, central Japan	6.7	DF	5F	27	0.5

Throughout the table, the asterisk indicates mean values and 'nd' indicates no data or not mentioned.

[a] CPF, Cold permafrost; WPF, warm permafrost; SF, seasonal frost; DF, diurnal frost; DT, diurnal thaw.

[b] T, Maximum thaw depth; F, maximum frost depth.

[c] Non-electoric methods: MS, marked stones; TR, tilting rods; PG, pegs (wood, plastic); CM, columns (wood, plastic, etc.); AF, aluminum foil strips; PT, plastic tubes. Electoric methods: IC, inclinometers; SP, strain probes; SM, solifluction meter.

[d] NIC, Needle ice creep; DFC, diurnal frost creep; AFC, annual frost creep; GF, gelifluction; PL, plug-like flow; ALG, active layer glide; MF, mudflow; TC, talus creep.

[e] SSP, Sorted stripes; NSP, non-sorted stripes; SBL, stone-banked lobes; TBL, turf-banked lobes; SBT, stone-banked terraces; TBT, turf-banked terraces; HK, hummocks; GS, grazing steps; SS, smooth slope; TL, talus slope.

[f] S, Stripe spacing; H, riser height.

Maximum heave (cm)	Surface velocity (cm year^{-1})	Depth of movement (cm)	Methods of measurement[c]	Major processes[d]	Landforms[e] (dimensions in cm)[f]	Reference
nd	0.3–3	nd	MS	GF	SBL	Harris et al. (1998)
nd	6.5 *	40–80	CM	AFC, GF, PL	TBL (100–150H), SBL, TBT	Gorbunov and Seversky (1999)
nd	3.0 *	nd	MS	DFC, GF	SBL	Sone et al. (1998)
nd	1.7	50	PG, CM	AFC, GF	TBL (50H)	Benedict (1970)
nd	2.2	nd	MS	GF	SSP (330S)	Benedict (1970)
21 *	1.0	50	PG, CM	AFC, GF	TBL (150H)	Benedict (1970)
nd	0.2	nd	PG	AFC	TBT (100H)	Benedict (1970)
nd	0.3	nd	MS	AFC	SBL (60H)	Benedict (1970)
nd	0.4	nd	MS	AFC	SBT (150H)	Benedict (1970)
nd	0.3	nd	PG	AFC	TBL (200H)	Benedict (1970)
nd	0.03	nd	MS	AFC	SSP (250S)	Benedict (1970)
nd	0.2	nd	PG	AFC	TBT ($<$ 120H)	Benedict (1970)
nd	25–49	nd	GD	nd	TBL	Zhu (1996)
nd	11.2 *	nd	TR	GF	TBL (70–400H)	Gengnian et al. (1995)
5.1	3.4 *	41	PT, SP	GF	SBL (40H)	This paper
1.5	1.3 *	21	PT, SP	DFC	SSP (20–30S)	This paper
2–5	0.5 *	33 *	IC, CM, MS	AFC	TBL (40H)	Smith (1988, 1992)
7	21 *	ca. 50	PP, SM	GF	TBL (10–50H)	Jaesche et al. (1997)
1.4–2.9	16.9 *	20	MS, SP	DFC, NIC	SBL (20H)	Matsuoka (1998b)
nd	25 *	8	MS, CM	NIC	SSP	Mackay and Mathews (1974)
nd	2.8 *	nd	MS	nd	TBT (57H)	Hansen-Bristow and Price (1985)
nd	100 *	18	MS, CM	NIC $\gg$ FC, GF	SBL (30H)	Francou and Bertran (1997)
nd	26 *	22	MS	DFC, NIC, GF, TC	SBL (30H), TBL, SSP (20S)	Sohma et al. (1979)
nd	4.1 *	38 *	CM, AF	AFC, GF	TBL (50H)	Gamper (1981, 1983)
nd	0.5–16	nd	MS	nd	nd	Pissart (1993)
nd	0.36	nd	CM	nd	TBT (140H)	Mark (1994)
nd	16.3 *	3–5	MS, PG, CM	NIC	SBT	Pérez (1987)
nd	6.0 *	5	MS	NIC	SSP (10S)	Pérez (1992)
ca. 10	15 *	10	MS, PT	DFC	SSP	Caine (1963)
5.8	25 *	12	MS, PT	NIC, DFC, GF	TBL	Sawaguchi and Koaze (1998)
nd	1.0 *	15	CM	FC	TBT	Ishii (1976)
6.3	3.4 *	32	PT	AFC, GF	TBL, HK, GS	Nakaya (1995)
2.5	0.3 *	4	PT	NIC	GS	Nakaya (1995)

freeze–thaw depth. Other significant parameters include the mean annual ground temperature, freeze–thaw frequency and soil moisture content, but the sparseness of information in the literature does not allow data analysis.

MAAT is not always cited in the literature. In the absence of data, MAAT was simply estimated from meteorological data at a nearby weather station, using a lapse rate of 6°C km^{-1}. An error can arise from this approximation, but is unlikely to be greater than $\pm$2°C. The estimated values are indicated in Tables 1 and 2 with the symbol '$\sim$'. MAAT at the measurement sites ranges from $-$19°C (the Canadian Arctic) to 7°C (hillslopes in Japan). Sites with

MAAT > 3°C are largely located below the regional treeline.

The frost type is classified into permafrost, seasonal frost and diurnal frost. Permafrost is subdivided into cold permafrost and warm permafrost, which effectively correspond to continuous and discontinuous permafrost, respectively. In terms of solifluction, however, the local frost condition, which reflects permafrost temperature, is more relevant than the regional continuity of permafrost. Similarly, slopes located in the sporadic permafrost zone may be classified as either warm permafrost or seasonal frost. For sites where frost type is not identified in the literature, cold permafrost is evaluated by MAAT < -6°C and seasonal frost by MAAT > -3°C, on the basis of the empirical relationships obtained from the identified sites. Diurnal frost is distributed on slopes dominated by diurnal freeze–thaw cycles and lacking seasonal frost or thaw penetration. This occurs on many tropical high mountains devoid of seasonal change in temperature (Pérez, 1987, 1992; Francou and Bertran, 1997), below the seasonal frost zone on mid-latitude mountains, and on very cold mountains in Antarctica (Matsuoka and Moriwaki, 1992).

The freeze–thaw penetration depth delimits the extent to which solifluction can occur. The maximum annual frost depth D_F for non-permafrost sites and thaw depth D_T for permafrost sites are cited in Tables 1 and 2, if the value is available. Both D_F and D_T range from a few centimeters in the diurnal frost zone to 2–3 m near the borderline between the seasonal frost and warm permafrost zones.

3.3. Process parameters

3.3.1. Frost heave

Soil movement consists mainly of components normal to the slope (frost heave) and downslope (solifluction). Frost heave was measured concurrently with solifluction at a number of localities. Many researchers estimated the heave amount by upfreezing of a stake, thereby recording cumulative heave. This method is of low accuracy, because partial subsidence of the stake can occur on temporary thawing. Some data resulted from bedstead measurements that provide differential movement between the ground surface and a fixed point at depth, and therefore the accuracy is higher. In particular, where recording is automated, this methodology can detect multiple heave events in a year (Smith, 1988; Matsuoka and Moriwaki, 1992; Nakaya, 1995; Sawaguchi, 1995; Jaesche et al., 1997; Matsuoka et al., 1997; Matsuoka, 1998a; Sawaguchi and Koaze, 1998). The values cited in Tables 1 and 2 for these publications show the maximum annual heave amount: where only seasonal heave occurs, the value indicates the seasonal heave amount; and where diurnal heave cycles are significant, it represents the largest heave event in a year. In the latter case, this value considerably underestimates the annual total of individual heave amounts.

3.3.2. Downslope movement

A variety of methods have been applied to measure solifluction (Tables 1 and 2). Surface displacement can be determined with painted lines, marked stones, tilting rods and pegs. These methods may yield slightly different velocities on the same slope, because the first two indicate the movement of the uppermost particle, while the last two, partially buried in the ground, reflect the movement of the uppermost soil layer. Cumulative displacement is usually provided by measurements at intervals. The subsurface velocity profile is evaluated by the deformation of a sensor (either electric or non-electric) installed in the ground. Whereas all of the non-electric sensors (e.g., wooden columns, aluminum foil strips and plastic tubes) need re-excavation of the ground, the electric sensors (e.g., inclinometers, strain probes and solifluction meters) can indicate subsurface movement without excavation. In particular, the combination of an electric sensor with a data logger permits year-round, automatic recording (e.g., Lewkowicz, 1992b; Matsuoka, 1994; Jaesche et al., 1997; Yamada et al., 2000). The intersection of these subsurface sensors with the ground surface also indicates the surface displacement.

Downslope movement is defined by the three parameters, the surface velocity V_S, volumetric velocity V_{VL} and maximum depth of movement D_M (Fig. 3). V_S represents the mean annual downslope displacement of the surface particles. V_{VL} shows the annual soil volume passing through a unit width (1 cm), having a dimension of $cm^3\ cm^{-1}\ year^{-1}$. D_M indicates the base of the detectable movement. Ta-

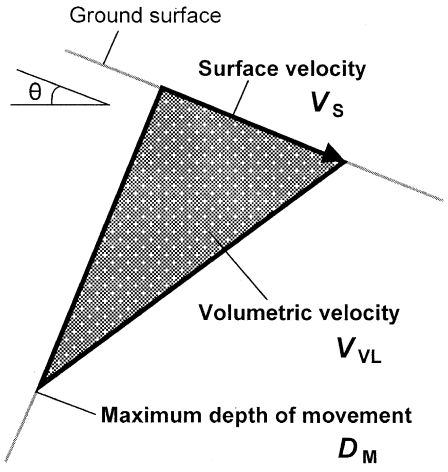

Fig. 3. Soil movement parameters.

bles 1 and 2 list data of V_S and D_M. V_S is highly variable but most frequently of the order of cm year^{-1}. D_M rarely exceeds 70 cm. Some publications cite V_{VL} values (12 sites). An illustration of a velocity profile also permits the estimation of V_{VL} (15 sites). If both the V_{VL} value and illustration are absent but V_S and D_M are available, V_{VL} was simply estimated by $1/2V_S D_M$, on the assumption of a linear decrease in velocity with depth (four sites).

The accuracy of measurement depends partly on the length of the monitoring period, in addition to the methodology. This is because inter-annual variability in velocity can arise from climate fluctuation (e.g., Åkerman, 1996). Furthermore, sensor installation accompanied by significant disturbance of soil tends to result in faster movement during the first few years (Smith, 1992). Thus, minimum soil disturbance (e.g., by using an auger with a small diameter) or long-term monitoring provides more accurate results. The actual monitoring periods range from one winter to more than 30 years, with a mode of 2–5 years (Tables 1 and 2).

Tables 1 and 2 also display the major process types operating on the slope. The listed processes basically follow the opinion of the original authors. However, some references lack a clear statement of the processes operating. In such cases, the prevailing processes were evaluated from the data description. Some solifluction slopes also undergo processes not involved in solifluction, such as mudflows and active layer glides, which are also noted.

4. Climate and movement

4.1. The effect of the mean annual air temperature

The three movement parameters (V_S, V_{VL} and D_M) vary significantly with MAAT (Fig. 4). A data point in Fig. 4 basically represents the mean value for a study site, except where data are summarized for each landform type. The surface velocity V_S is very low, rarely in excess of 5 cm year^{-1} on slopes with MAAT < -6°C, where permafrost is largely cold and continuous. V_S rises with increasing MAAT,

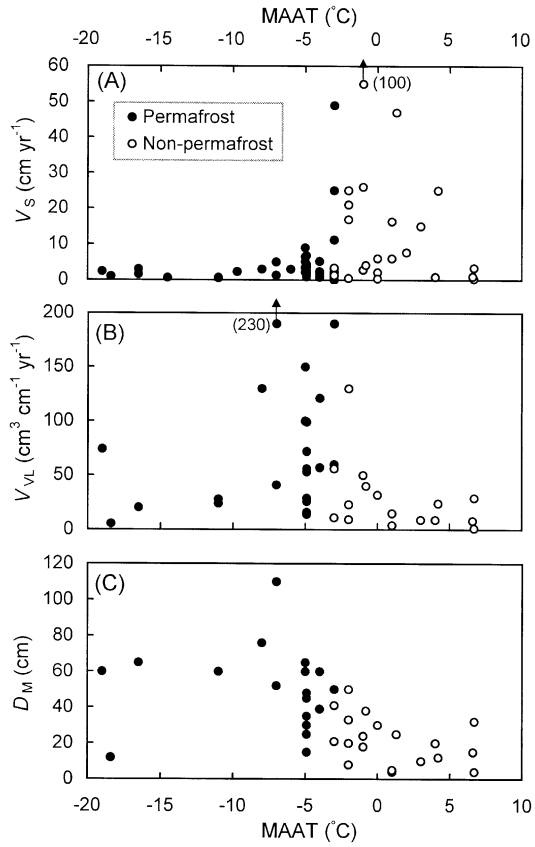

Fig. 4. Periglacial soil movement as a function of the mean annual air temperature (MAAT). See Fig. 3 for definitions of V_S, V_{VL} and D_M.

reaching a maximum in a zone with MAAT between −3°C and −5°C (Fig. 4A). Within this optimum zone, V_S often exceeds 10 cm year^{-1}. This zone includes both slopes underlain by warm permafrost (temperature of which is close to 0°C) and those lacking permafrost. However, high V_S values are unlikely to result from the presence of permafrost or deep seasonal frost. In fact, V_S in excess of 10 cm year^{-1}, which occurs mostly on mid- to low-latitude high mountains, is usually associated with a high frequency of diurnal freeze–thaw cycles.

In contrast, the maximum depth of movement D_M is largest (~60 cm) in the cold permafrost zone, decreasing toward the non-permafrost zone (Fig. 4C). A cold permafrost slope (MAAT = −18°C) indicates shallow movement (D_M = 12 cm), but this is an exceptional site in Antarctica where the active layer is confined to the uppermost 15 cm (Matsuoka and Moriwaki, 1992). The deepest movement (D_M = 110 cm) was recorded in Svalbard (Fig. 2D; Matsuoka and Hirakawa, 2000). D_M ranges from a few centimeters to 50 cm in non-permafrost areas.

The spatial variation in the volumetric velocity V_{VL} reflects the integration of V_S and D_M (Fig. 4B). V_{VL} reaches a maximum in the warm permafrost zone, often in excess of 100 cm^3 cm^{-1} year^{-1}, decreasing toward both the cold permafrost and seasonal frost zones. This indicates that solifluction produces the most rapid denudation where slopes are underlain by warm permafrost.

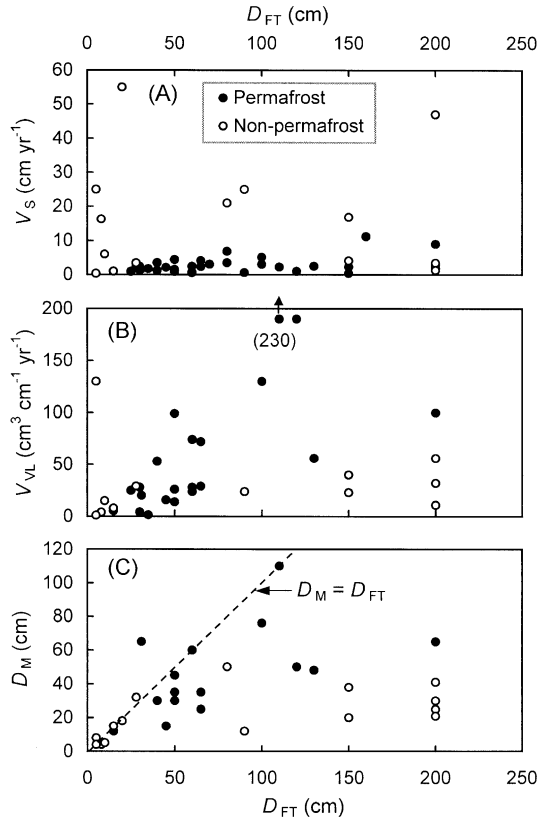

Fig. 5. The influence of the annual freeze–thaw depth D_{FT} on solifluction. See Fig. 3 for definitions of V_S, V_{VL} and D_M.

4.2. The effect of freeze–thaw depth

The maximum annual freeze–thaw depth D_{FT}, which represents D_F in non-permafrost sites and D_T in permafrost sites, contributes to soil movement in the two environments in slightly different ways (Fig. 5). At non-permafrost sites, D_F rarely influences V_S (Fig. 5A); D_M nearly equals D_F, where $D_F < 30$ cm, but does not rise consistently with deepening frost penetration, reaching the upper limit at ~50 cm, where $D_F > 50$ cm (Fig. 5C). Similarly, V_{VL} also approaches the upper limit at ~50 cm^3 cm^{-1} year^{-1} (Fig. 5B), except for a mountain slope in British Columbia, where the downslope convexity of a velocity profile arises from shallow but extraordinary rapid movement (Mackay and Mathews, 1974).

At the permafrost sites, by comparison, V_S is generally low, but rises slightly with D_T (Fig. 5A). Both V_{VL} and D_M are also roughly in proportion to D_T (Fig. 5B and C). D_M on some slopes accords with the base of the active layer. A High-Arctic slope experiences movement in the upper part of permafrost as well as solifluction in the active layer, resulting in $D_M > D_T$ (Bennett and French, 1991; see also Fig. 5C).

4.3. Discussion: climatic controls on solifluction

The key factors controlling the above relationships are considered to be, first, the depth of ice lens formation at which displacement can occur on thawing and, second, the freeze–thaw frequency. The roles of these factors are evaluated below on the

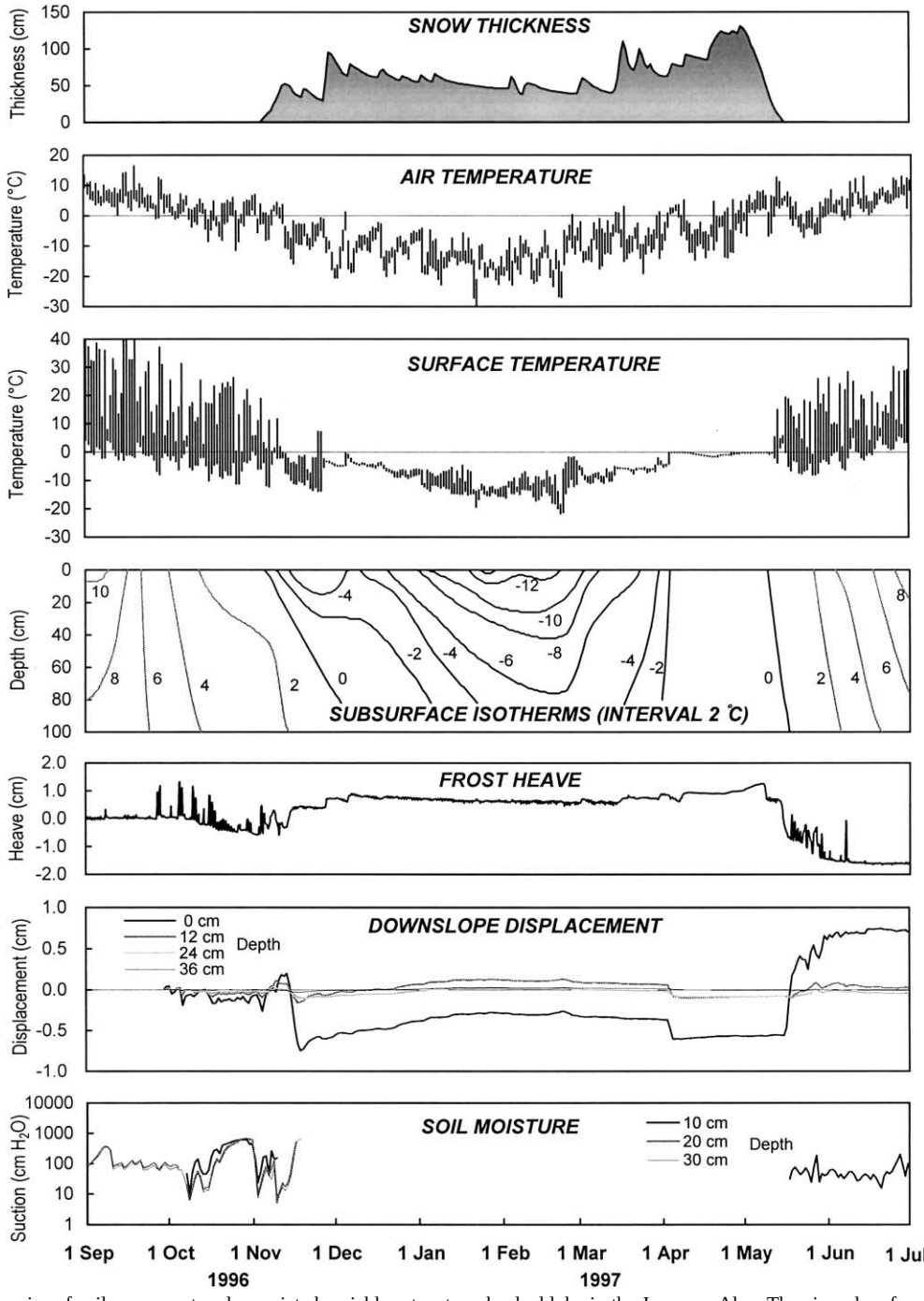

Fig. 6. Time series of soil movement and associated variables at a stone-banked lobe in the Japanese Alps. The air and surface temperatures are displayed as daily ranges. Downslope displacement is indicated by positive values. Diurnal frost heaving and resulting soil creep prevailed, while seasonal heave was of similar magnitude to some of the large diurnal heave events. Note that seasonal frost heave in the winter produced an apparent upslope movement of a strain probe, which was offset on thawing. Reproduced with permission from Matsuoka (1998b), © 1998 John Wiley & Sons Limited.

basis of detailed solifluction observations combined with monitoring of ground thermal regimes and frost heave activity.

As regards the first factor, year-round monitoring on a Japanese alpine slope revealed that, despite seasonal frost penetration to a depth of ~2 m, D_M is not deeper than 20 cm (Fig. 6). Such a shallow movement originates from the thin superficial layer of frost-susceptible fine soil (containing considerable silt and clay) which responds mainly to diurnal frost heave activity; movement rarely occurs in the non-frost susceptible block layer or bedrock at depth, to which only seasonal freezing penetrates (Matsuoka, 1998b). The non-frost susceptible nature of the deeper layer is also documented by the very small seasonal frost heave (Fig. 6). In the Swiss Alps, similar shallow movement is observed on a crest slope that displays small-scale sorted stripes (spacing at 20–30 cm) and lacks a thick fine layer (Fig. 2A), while deeper movement ($D_M \approx 50$ cm) occurs on a lower slope where fine sediments accumulate to a depth of 2 m or more, producing stone-banked lobes (Fig. 2B). Soil deformation occurring at 20–50 cm depth at the latter slope is likely to follow the large seasonal heave (~5 cm), although D_M is still much shallower than the maximum frost penetration, which extends deeper than 1 m (Fig. 7; see also Matsuoka et al., 1997 for additional data). Such a difference between D_M and D_F originates, firstly, from desiccation of the subsoil as a result of ice segregation in the upper layer and resulting lack of ice lenses in the lower part of the seasonally frozen layer. In addition,

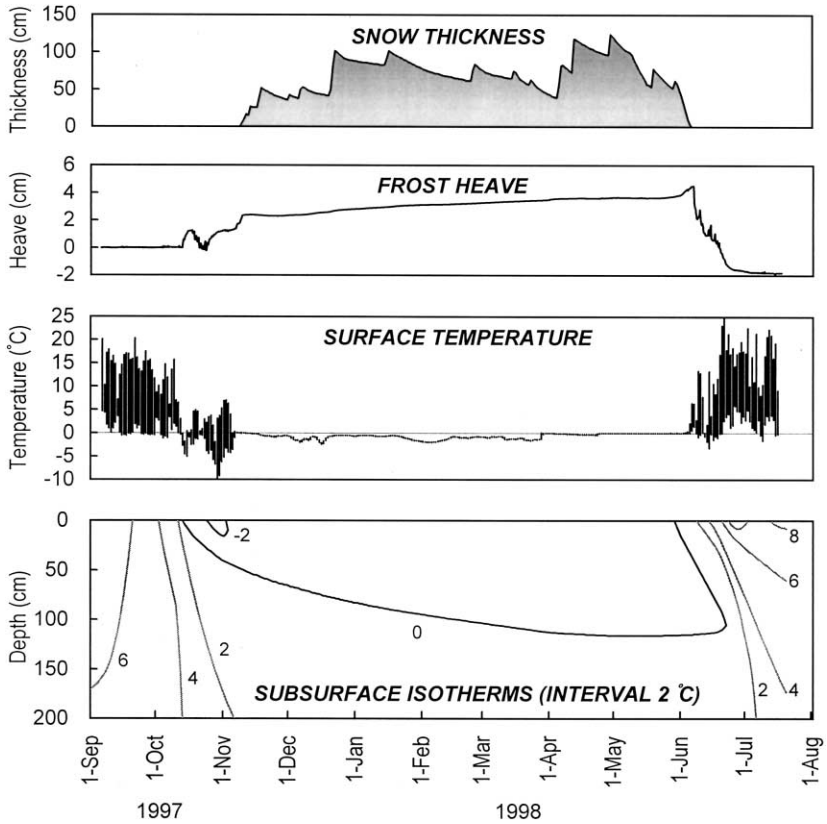

Fig. 7. Frost heave and climatic variables at a stone-banked lobe in the Swiss Alps. In contrast to the infrequency and small magnitude of diurnal frost heave cycles, seasonal heave amounted to 4.5 cm, suggesting that annual frost creep or gelifluction is largely responsible for the soil movement recorded in tubes (see Fig. 2B). Note that partial penetration of the heave sensor in the soft thawed layer caused an apparent subsidence of the ground on seasonal thawing.

as suggested by a laboratory study (Harris and Davies, 2000), even if ice lenses occur throughout the frozen layer, decreasing void ratio and increasing shear strength during thawing may prevent gelifluction in the lower layer.

Conditions differ significantly in polar regions. For example, observations showed contrasting subsurface movement at two sites in Svalbard (Matsuoka and Hirakawa, 2000). Typical solifluction movement, similar to that on the stone-banked lobe in the Swiss Alps, occurs on a coastal turf-banked sheet underlain by permafrost (Fig. 2C). Excavation in summer revealed that the active layer, composed of fine sediments, reaches 130 cm depth, but movement is confined to the uppermost 50 cm. In contrast, D_M corresponds to the bottom of the active layer at 110 cm depth on an upland slope with wide non-sorted stripes (spacing at 2.5 m) (Fig. 2D). Excavation to the base of the frozen active layer showed a number of ice lenses 1–2 mm thick just below the thawing front (between 90 and 110 cm depth) in the early summer; they probably developed during upfreezing from the permafrost table at ~110 cm depth. Soil movement occurs in zones at 40–60 and 90–110 cm deep, probably reflecting frost heaving by two-sided seasonal freezing indicative of cold permafrost. The seasonal heave amounted to ~5 cm (Fig. 8). The slightly different thermal conditions between the two sites in Svalbard, corresponding to ~2°C in terms of MAAT, are likely to result in the differing permafrost temperatures and frost heave characteristics. These observations suggest that the prevailing freeze–thaw type, subsurface thermal regime and soil characteristics combine to control the depth and thickness of ice lenses which, in turn, influence movement indices.

Freeze–thaw frequency mainly affects the velocity of the superficial layer. As mentioned above, high V_S values occur on mid- to low-latitude mountains that experience 10^1–10^2 diurnal freeze–thaw cycles annually. For instance, the highest velocity (100 cm year^{-1}) originated from a tropical high mountain undergoing shallow but frequent diurnal freezing (Francou and Bertran, 1997). Concurrent monitoring of soil heave, downslope movement, moisture and temperature demonstrate that the repetition of frost heave cycles, fed by the temperature cycling across 0°C and periodic moisture supply, promotes soil creep (needle ice creep and diurnal frost creep) in the top 15 cm of soil on such alpine slopes (Matsuoka, 1998a; see also Fig. 6). The depth of ice lens formation varies with the intensity of nocturnal cooling,

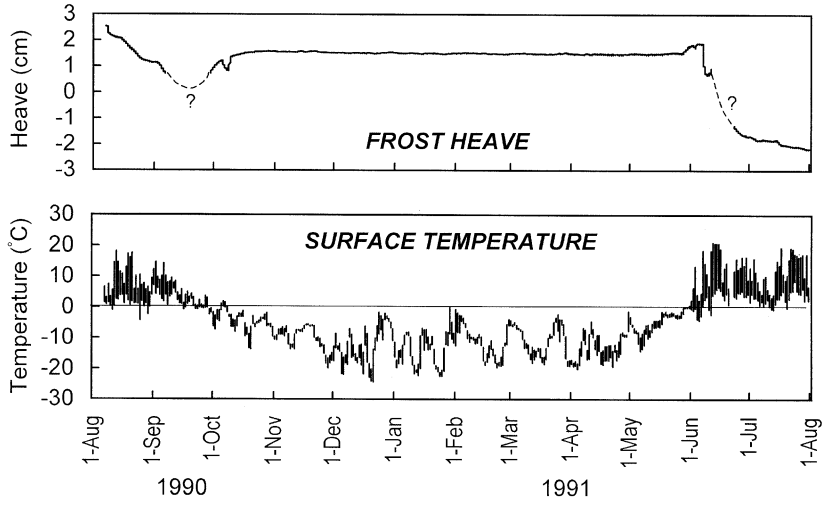

Fig. 8. Frost heave and surface temperature records at a non-sorted stripe site in Svalbard. Data indicate the rarity of diurnal frost heaving and the predominance of seasonal frost heaving. Because the bedstead to which the heave sensor has attached itself upheaved by 3.4 cm during the year, the actual seasonal heave amounted to ~5 cm. Deformation of tubes (Fig. 2D) suggests that the seasonal heave accompanied two-sided freezing.

from a few millimeters (i.e., needle ice) to ~15 cm, most frequently lying within the top 5–10 cm. The resulting velocity profile generally displays downslope concavity. Mountain slopes subject to both diurnal and seasonal frost heaving experience deeper movement that still shows downslope concavity (see Fig. 2B). In general, velocity profiles showing downslope convexity increase poleward (e.g., Mackay, 1981; Price, 1991) in response to declining diurnal frost heaving and prevailing seasonal frost heaving (Fig. 8). It is worth noting, however, that a vegetation mat reduces V_S by acting as a thermal insulator that lowers freeze–thaw frequency and by contributing to surface resistance to movement through its binding effect on near-surface soil. As a result, a convex downslope velocity profile can occur even on mid-latitude mountains (e.g., Benedict, 1970; Smith, 1992).

Alpine slopes contrast with polar slopes also by the difference between V_S values given respectively by surface and near-surface markers (Fig. 9). Painted surface particles move downslope much faster than the tops of flexible tubes installed on alpine slopes (e.g., Andes and Japan), because only the former respond to needle ice creep (Matsuoka, 1998a). Moreover, since the response to needle ice creep depends on the grain size of the uppermost layer, the spatial variation in surface texture leads to a variable velocity distribution in plan (e.g., Mackay and Mathews, 1974; Pérez, 1988; Matsuoka, 1998b). On polar slopes (e.g., Svalbard), in contrast, surface particles and the tops of tubes yield nearly equal V_S values (Sawaguchi, 1995). Surface and near-surface markers also indicate similar velocities in the Canadian Arctic (Egginton and French, 1985). Data from the Rockies (Benedict, 1970; Smith, 1988) are similar to those from polar slopes (Fig. 9), but this seems to be due to the vegetation mat that hinders needle ice creep. Another feature of polar slopes is that a row of surface markers usually displays parallel dislocation regardless of the variation in the surface texture (e.g., Washburn, 1967; Sawaguchi, 1995), probably because movement largely reflects seasonal frost heaving at depth.

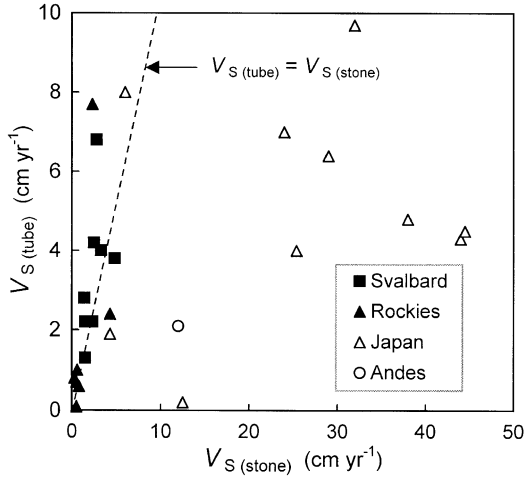

Fig. 9. Difference between surface velocity, indicated by surface stones $V_{S\,(stone)}$ and the tops of flexible tubes $V_{S\,(tube)}$. Data are from Svalbard (Sawaguchi, 1995), Rockies (Benedict, 1970; Smith, 1988), Japan (Matsuoka, 1998b) and Andes (Pérez, 1987).

A final remark concerns the factors potentially contributing to obscure the relationships in Figs. 4 and 5. The most significant factors include the fine debris composition (as already mentioned), moisture status and slope gradient. The climate-related factor, moisture status, influences solifluction both spatially and temporally, reflecting precipitation and snow distribution. For instance, a late-lying snow patch behind a solifluction lobe supports a high water level until the seasonal freezing period; the resulting large heave in winter is responsible for large annual frost creep and gelifluction in the following summer (Benedict, 1970). The addition of rain or meltwater during seasonal thawing also raises the moisture content of a thawing slope, possibly promoting gelifluction (Harris, 1972; Smith, 1988), or even producing rapid flows or slides on slopes in excess of 20–25° (Harris, 1981). A intra-site variation in soil moisture affects V_S values on continuous permafrost slopes (Washburn, 1967, 1999), possibly by controlling the occurrence of plug-like flow near the base of the active layer. Temporal variation in diurnal frost creep velocity may result from the seasonal humidity change (e.g., Francou and Bertran, 1997) or cyclic precipitation (e.g., Matsuoka, 1996). Despite such a number of observations, however, more detailed, quantitative data are required in order to describe the rate of solifluction as a function of moisture status. The effect of slope gradient is examined in the next section.

5. Topography and movement

5.1. The effect of inclination

The dependence of movement on inclination has been described in several mathematical models. The simplest model gives the surface velocity V_S by:

$$V_S = H_F \tan\theta \quad (1)$$

where H_F is the heave amount perpendicular to the slope surface and θ is the slope angle (e.g., Williams and Smith, 1989). For slopes subject to multiple frost heave cycles, Eq. (1) is rewritten as:

$$V_S = \sum H_F \tan\theta \quad (2)$$

where V_S gives the annual surface velocity and $\sum H_F$ the annual total heave amount. V_S in Eqs. (1) and (2) is also called the potential frost creep. In reality, soil cohesion yields some retrograde movement that reduces V_S (Washburn, 1979). Where needle ice activity prevails, rotational movement or toppling of ice needles intensifies the effect of inclination such that:

$$V_S = C\sum H_F \tan^2\theta \quad (3)$$

where C is a constant (Higashi and Corte, 1971; Matsuoka, 1998b).

Increasing solifluction rates with inclination have been reported from some polar mountains, such as the Canadian Arctic (Washburn, 1967) and Svalbard (Åkerman, 1996; Sawaguchi, 1995). In Iceland, Hirakawa (1989) also found a similar relationship between inclination and the long-term mean rates estimated from the tephrostratigraphic evidence. In the lower-latitude alpine areas, however, the influence of inclination is often masked by the spatial variation in other factors like freeze–thaw frequency, surface texture and moisture distribution (e.g., Benedict, 1970; Harris, 1981), although Pérez (1987) found a rough correlation between rate and inclination on slopes dominated by needle ice creep.

Available field data are plotted on the inclination–velocity diagram (Fig. 10). Each point in this diagram represents data for an individual plot, because velocity varies widely with inclination within a study site. Where an individual value is not available, a point indicates the mean value for a site. Examination of this diagram should segregate two groups of sites: those governed by diurnal freeze–thaw action (where needle ice creep may prevail) and the rest, because Eqs. (2) and (3) suggest different responses to inclination. For both groups, and irrespective of the presence of permafrost, only a weak correlation is found between V_S and tan θ (Fig. 10A). However, there appears to be a maximum V_S for a given inclination. Apart from the sites dominated by diurnal freeze–thaw action, this maximum is approximated by the line:

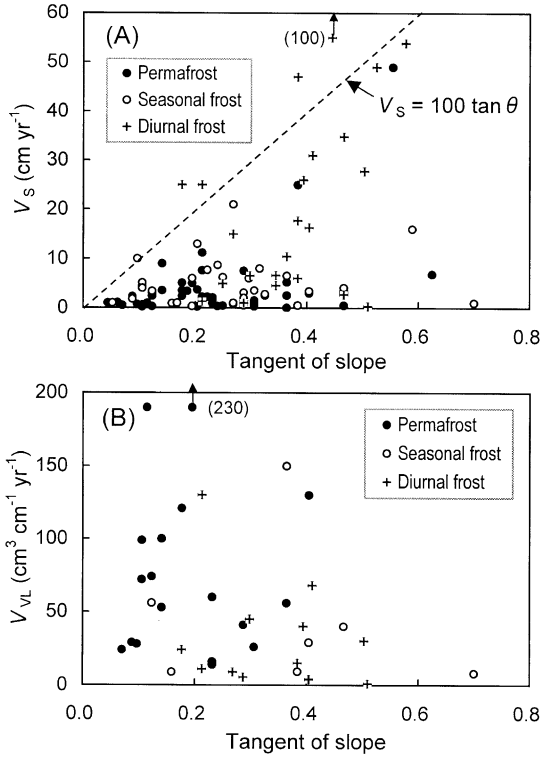

Fig. 10. Solifluction rates as a function of the slope gradient. See Fig. 3 for definitions of V_S and V_{VL}.

$$V_S = 100 \tan\theta \quad (4)$$

where the dimension of V_S is cm year^{-1} and θ is in degrees. In terms of the potential frost creep model (Eqs. (1) and (2)), this equation suggests that the seasonal frost heave or annual total heave amount does not exceed 100 cm. In fact, field observations have reported a heave amount up to several decimeters (e.g., Benedict, 1970; Matsuoka, 1998a). Some

slopes exposed to a high freeze–thaw frequency have recorded V_S values higher than those given by Eq. (4) (Fig. 10A), which probably reflects toppling or rolling of particles lifted by needle ice.

The dependence of V_{VL} on inclination is less clear (Fig. 10B). There appears to be a weak trend for V_{VL} to decrease with inclination. A possible factor governing this trend is the thickness of frost-susceptible fine debris. Steep slopes cannot hold a thick layer of fine debris that is readily removed, whereas downslope declination allows sedimentation of the fine debris on the lower slopes. The resulting downslope increase in D_M, possibly aided by a rise in moisture availability, may lead to increasing V_{VL} despite declination. This implies that, in addition to inclination, the slope form (e.g., concave, convex or irregular) contributes indirectly to the rate and process of solifluction, by affecting the debris thickness, snow distribution, drainage condition and microclimate.

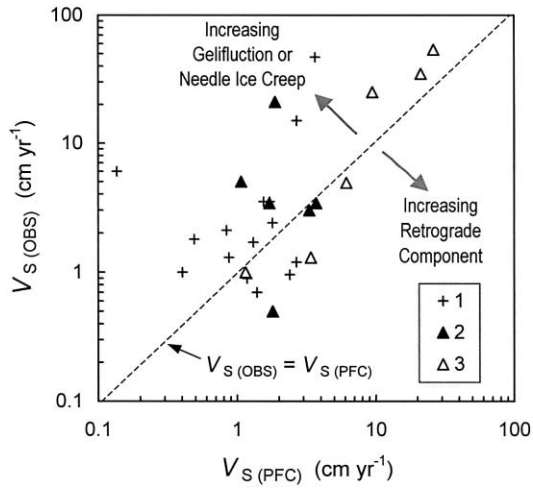

Fig. 11. Potential frost creep $V_{S\,(PFC)}$ computed from frost heave amount versus observed surface velocity $V_{S\,(OBS)}$. Legends: 1—Heave measured manually; 2—Heave measured automatically, annual freeze–thaw action dominant; 3—Heave measured automatically, diurnal freeze–thaw action dominant.

5.2. Discussion: potential frost creep versus actual movement

The deviation of the observed velocity from potential frost creep is a useful indicator of the prevailing solifluction component. For example, based on a large-scale laboratory freeze–thaw experiment, Harris et al. (1993) found that the ratio of frost creep to gelifluction varies significantly with the fine debris content of soils. A number of field studies have also compared the actual movement with potential frost creep (Washburn, 1967; Benedict, 1970; Harris, 1972; Smith, 1987a; Bennett and French, 1991; Matsuoka, 1998a). However, the estimation of potential frost creep is of low accuracy when frost heave is manually measured with stakes, because this methodology fails to detect some partial subsidence of the ground surface on temporary thawing. This may cause significant underestimation of the annual heave amount, in particular, where diurnal heave cycles occur frequently. Thus, more precise evaluation of potential frost creep requires the total heave amount derived from year-round continuous recording.

Fig. 11 compares the potential frost creep $V_{S\,(PFC)}$ with the actual velocity $V_{S\,(OBS)}$. Data points are sorted by the type of measurement (manual or automated) and prevailing freeze–thaw action. Note that $V_{S\,(OBS)}$ in this figure represents the specific value at the heave monitoring site, not the regional mean value. As a whole, data cluster around the line of $V_{S\,(OBS)} = V_{S\,(PFC)}$, suggesting the primary role of frost heave in causing downslope displacement. Data points displaced upper-leftward from this line indicate the predominance of gelifluction or needle ice creep, while those lower-rightward imply a significant retrograde component. As regards data based on automated measurements, the upper-left region includes six points, three of which originate from slopes governed by diurnal freeze–thaw action ($V_{S\,(OBS)} \approx 20$–60 cm year^{-1}). The three points were obtained from Japanese mountains where, in fact, high needle ice creep activity was reported (Matsuoka, 1998a; Sawaguchi and Koaze, 1998). The other three data ($V_{S\,(OBS)} \approx 3$–20 cm year^{-1}) are associated with seasonal frost heaving of 5 cm or greater that may result in a large gelifluction component on thawing; they include two slopes having solifluction lobes in the Alps (Matsuoka et al., 1997; Jaesche et al., 1997) and one undergoing plug-like flow in Svalbard (Matsuoka and Hirakawa, 2000). Most of the calculated potential frost creep values based on the manual measurement underestimate the

actual velocity (Fig. 11). Previous interpretations have attributed this to the predominance of gelifluction, but the contribution of diurnal frost creep seems to have been neglected at some sites.

The analysis based on potential frost creep so far only permits an inter-site comparison of the relative magnitude of each component. Quantitative evaluation of the ratio of each component requires the determination of the retrograde movement induced by soil cohesion, which has yet to be successful.

6. Landforms resulting from solifluction

6.1. Movement of solifluction lobes

Lobes and sheets are surface expressions directly reflecting solifluction. They originate from overturning of the superficial soil due to reduced velocity and thus develop most extensively where gradient decreases downslope (Fig. 12) or where a fine soil layer overrides a coarse sediment (Fig. 2C). Typically, lobes consist of a riser 0.2–2 m in height and a tread 2–50 m in both width (measured along contours) and length (measured downslope) (e.g., Harris, 1981). Sheets have a similar height but their horizontal continuity makes the definition of the width and length difficult.

The V_S–D_M diagram (Fig. 13A) displays the two-dimensional movement for different lobe types. On turf-free stone-banked lobes, the predominance of diurnal freeze–thaw action results in shallow ($D_M \approx 20$ cm) but fast movement (needle ice creep or diurnal frost creep), while depressed diurnal and enhanced annual action is responsible for deeper ($D_M \approx 30$–50 cm) but much slower movement (annual frost creep or gelifluction). The presence of vegetation prevents diurnal frost creep and needle ice creep on turf-banked lobes irrespective of the occurrence of diurnal freeze–thaw cycles in air, highlighting annual frost creep or gelifluction which in most cases induces deep ($D_M \approx 30$–60 cm) and slow movement.

Such a difference in movement is reflected in the dimension of lobes. Fig. 13B demonstrates that deeper solifluction results in thicker lobes. The frontal height of lobe H_L is nearly equal to and sometimes greater than D_M. This implies that the maximum depth of movement determines the minimum frontal height. The height in excess of D_M is considered to reflect soil thickening toward the front, resulting from the caterpillar-like advance of soil mass and/or

Fig. 12. Turf-banked lobes in the Swiss National Park, developing where downslope declination and/or vegetation results in deceleration of movement. Detailed observations of these lobes were undertaken by Gamper (1981, 1983).

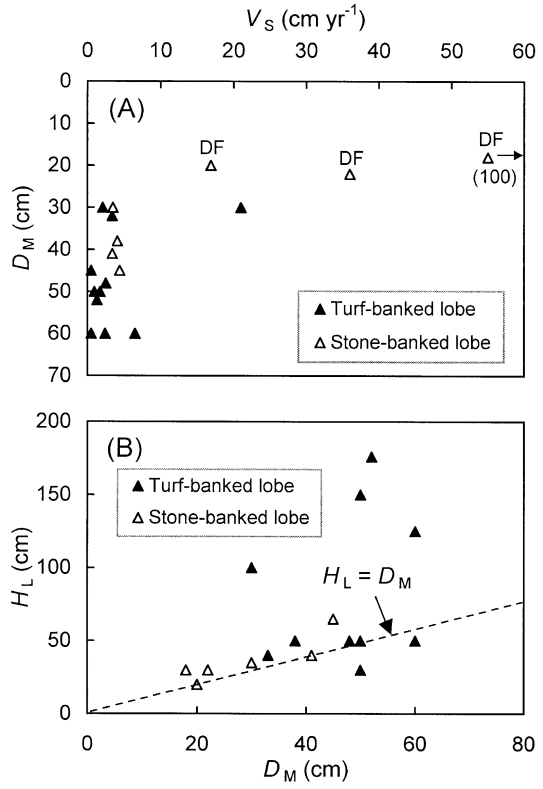

Fig. 13. Soil movement and resulting landforms. See Fig. 3 for definitions of V_S and D_M. Symbols: DF, diurnal frost dominant; H_L, frontal height of a lobe.

the deceleration of movement (e.g., Benedict, 1970; Gamper, 1981; Smith, 1988). The latter effect implies that V_S measured on the tread surface tends to overestimate the advancing rate of the solifluction lobe V_A. This overestimation is in fact shown by a comparison of V_S with the long-term mean V_A values estimated using time makers like buried organic layers or tephras (Table 3). The V_A values are commonly a few millimeters per year, that is, one order of magnitude smaller than the contemporary V_S values, although these two velocities are not dissimilar in some localities (Benedict, 1970; Smith, 1987b). Even the peak V_A values during the Late Holocene do not always exceed the contemporary V_S values.

6.2. Discussion: solifluction features as a climatic indicator

The above analysis implies that the frontal height of lobe is indicative of solifluction processes and microclimates. As the minimum H_L approximates D_M, measurements of H_L for smaller lobes on a slope give an estimate of D_M. In other words, H_L indicates the prevailing freeze–thaw action and frost depth, both influencing D_M. The height of inactive lobes or buried lobate structures can also be indicative of the past climate when the lobe was active.

Thin stone-banked lobes with $H_L \leq 20$ cm or smaller suggest the predominance of diurnal freeze–thaw cycles (e.g., Bertran et al., 1995), or fine soil confined within the uppermost 20 cm irrespective of the frost depth (e.g., Matsuoka, 1996). Stone-banked lobes with $H_L > 20$ cm and turf-banked lobes originate mainly from annual freeze–thaw cycles. In most cases, D_M (and also H_L) is considerably smaller than the maximum annual freeze–thaw depth D_{FT}, in response to the lack of fine soil at depth or desiccation of the lower layer in compensation for frost heave in the upper layer. If the near-surface fine

Table 3
Long-term advance rates of solifluction lobes

Site	Marker	Duration (year)	Mean rate (cm year^{-1})	Peak rate (cm year^{-1})	Reference
Iceland	Tephra	7000	0.1–0.2	0.3	Hirakawa (1989)
Okstindan, Norway	Organics	5500	0.2	–	Worsley (1993)
Jostedalsbreen, Norway	Organics	4000	–	0.2–0.7	Nesje et al. (1989)
Jotunheimen, Norway	Organics	1000	0.8	–	Matthews et al. (1986)
Swiss Alps	Organics	5000	–	3	Gamper (1983)
Brooks Range, AK	Organics	7000	0.3	–	Reanier and Ugolini (1983)
Ruby Range, Yukon	Organics	2500	0.6–1.0	–	Alexander and Price (1980)
Canadian Rockies	Organics	2000	0.5	1.5	Smith (1987b)
Colorado Rockies	Organics	2500	0.2	2.3	Benedict (1970)

soil is adequately thick and subject to continuous groundwater supply during seasonal freezing, D_M would approach D_{FT}, although data supporting this are rare. Where permafrost is cold enough to produce upward freezing, D_M approaches D_T (e.g., Mackay, 1981). The predominance of thick lobes (> 60 cm) may thus indicate the continuous moisture availability during seasonal freezing or the occurrence of two-sided freezing followed by plug-like flow, although plug-like flow occurs also on slopes lacking lobate features (Lewkowicz and Clarke, 1998; Matsuoka and Hirakawa, 2000).

Dimensions of other small-scale features on periglacial slopes can also be potential indicators of climate. For instance, spacing of sorted stripes developing on slopes varies from 10–30 cm in regions dominated by diurnal freeze–thaw action to > 200 cm where annual freeze–thaw action prevails (see Tables 1 and 2), which is proportional to the magnitude of D_M. This correspondence probably reflects that the spacing is a function of the depth of sorting which, in turn, depends on the freeze–thaw depth (e.g., Kranz, 1990). Understanding of such a linkage between climate and morphology, however, requires further process monitoring in diverse periglacial environments.

7. Synthesis

7.1. Contemporary solifluction

The freeze–thaw regime, soil characteristics, moisture status and topography are the major controls on solifluction features in modern periglacial environments. Fig. 14 illustrates how the first two

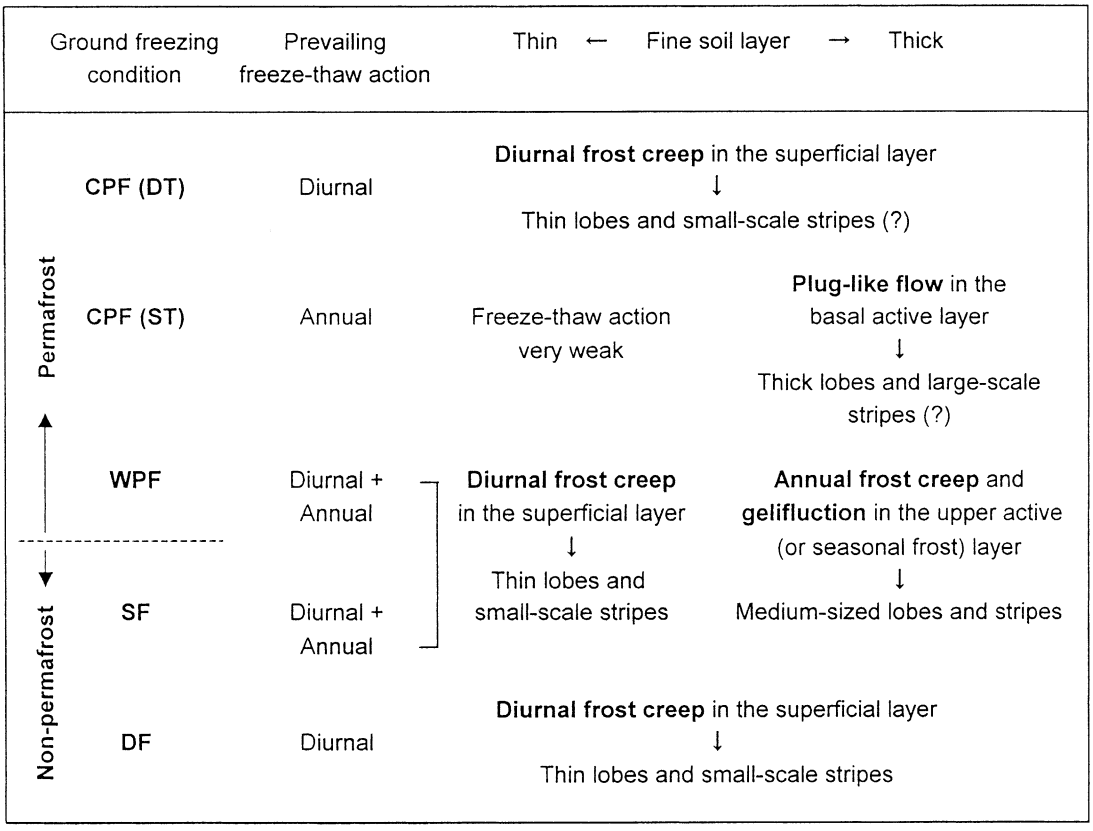

Fig. 14. Freeze–thaw regimes and solifluction. Frost types: CPF (DT), cold permafrost with diurnal thaw; CPF (ST), cold permafrost with seasonal thaw; WPF, warm permafrost; SF, seasonal frost; DF, diurnal frost.

factors contribute to the spatial variation in solifluction processes and landforms. Solifluction can operate where the uppermost soil encounters at least a diurnal freeze–thaw cycle. Thus, in term of the global thermal regime, the solifluction-affected environment is delimited by both warm and cold margins. Several sub-environments are identified in between.

The warm margin ranges from the mid-latitude lowlands to tropical uplands, where needle ice activity occurs only in mid-winter (see Lawler, 1988, for the global distribution). Just inside the warm margin, needle ice creep and diurnal frost creep resulting from short-term (diurnal and occasional cyclonic) freeze–thaw cycles dislocate the uppermost soil layer not deeper than 20 cm, creating thin lobes and small stripes, the height or spacing of which is commonly a few decimeters (e.g., Mackay and Mathews, 1974; Boelhouwers, 1995). These processes also contribute to raising rates of soil erosion in winter (e.g., Maekado and Matsukura, 1985; Lawler, 1986). Located far below the normal treeline, the distribution of such a diurnal frost environment in temperate regions requires a natural or artificial clearance of vegetation. The absence of seasonality provides a diurnal frost environment also on tropical high mountains, such as the Andes (e.g., Graf, 1976; Pérez, 1992), central Africa (Hastenrath, 1973) and Hawaii (Noguchi et al., 1987), where small-scale lobes, terracettes and stripes are widespread; the year-round occurrence of diurnal frost induces shallow but rapid soil movement that eventually leads to well-defined forms.

Increasing winter severity toward higher latitudes and altitudes permits seasonal frost penetration to several decimeters or more. Accordingly, slopes undergo both diurnal and annual freeze–thaw action. Such a seasonal frost environment is most widespread above the treeline on mid-latitude high mountains, where the winter frost typically reaches 1–2 m deep in the soil (e.g., Fahey, 1974; Matsuoka et al., 1997). In this environment, the thickness of fine soil, the snow distribution and drainage conditions modify freeze–thaw action. Near the crest of alpine slopes, regolith is usually thin and susceptible mainly to diurnal freeze–thaw action (needle ice creep and diurnal frost creep), because a large part of seasonal frost penetration occurs in a coarse blocky layer or bedrock (e.g., Matsuoka, 1998b). Even if the regolith is thick, good drainage may restrain seasonal frost heaving. The resulting lobes and patterned ground are generally small, of similar dimensions to those developed in the diurnal frost zone. Toward foot slopes, thickening of fine sediments, aided by poor drainage, intensifies annual freeze–thaw action (annual frost creep and gelifluction) (e.g., Matsuoka et al., 1997), resulting in larger lobes and terraces with a riser of 30–200 cm in height (Tables 1 and 2; see also Fig. 12). The superimposition of diurnal on annual freeze–thaw action may result in complex forms, for example, stripes within stripes (Hall, 1983) and smaller lobes on the tread of a large stone-banked lobe, although some of these forms are thought to reflect two stages of activity (Benedict, 1970; Boelhouwers, 1994). Alternatively, the effect of annual freeze–thaw action may prevail such that 'soupy' gelifluction enhanced by snow melt in spring obscures the smaller forms that may be produced during the autumn freeze–thaw period. Shallow seasonal frost to a few decimeters depth occurs also on forested hillslopes below the treeline, causing annual frost creep to be much larger than soil creep during the frost-free period (e.g., Auzet and Ambroise, 1996; Yamada, 1997).

Permafrost may encourage annual frost creep and gelifluction by improving moisture availability during seasonal freezing. Some observations in the warm permafrost zone in fact show large seasonal frost heave which raises potential frost creep (Benedict, 1976). However, Figs. 4 and 5 do not display any dramatic change in solifluction rates across the permafrost limit. This may partly reflect the near-crest locations of a number of monitoring sites, where thin regolith and free drainage minimize the effect of permafrost as a moisture barrier. Furthermore, gelifluction in spring may be intensified by inflowing snowmelt water over frozen subsoil even in some non-permafrost sites (e.g., Harris, 1972; Smith, 1988). Consequently, there seem to be insignificant differences in solifluction processes and resulting landforms between the seasonal frost and warm permafrost zones (Fig. 14).

Further poleward, both thinning of the active layer and lowering permafrost temperatures occur. Thaw penetration in summer produces an active layer several decimeters deep. Located mainly in polar re-

gions, such a cold permafrost environment experiences a very short autumn and prolonged snow cover until early summer. This condition is unfavorable for the occurrence of diurnal frost and thus allows the predominance of annual freeze–thaw action (see Fig. 8). In addition, where the whole active layer consists of fine soil and the moisture supply and/or poor drainage keeps the basal part of the active layer wet, upward freezing can produce ice lenses just above permafrost. The resulting plug-like flow leads to deep soil movement that may be responsible for large lobes and hummocks (Mackay, 1981; Gorbunov and Seversky, 1999).

Finally, around the cold margin of the solifluction environment (e.g., nunataks in Antarctica), only diurnal freeze–thaw action can operate in summer, dislocating the uppermost 10–15 cm of regolith (Matsuoka and Moriwaki, 1992). Because of the hyper-aridity of such nunataks, solifluction is only active on slopes receiving snowmelt water. Downslope movement occurs mainly as diurnal frost creep, not as needle ice creep, since near-surface cold permafrost promotes nocturnal freeze-back of the active layer before needle ice develops just below the surface grains. Diurnal frost creep may produce thin lobes or small sorted stripes as in the tropical high mountains, although these features have so far been rarely reported to date (cf. French and Guglielmin, 1999).

7.2. Possible effects of climate change on solifluction

Climate change influences solifluction by controlling the thermal and moisture regimes near the ground surface (e.g., Woo et al., 1992). Long-term warming or cooling may change the ground freezing condition, which affects solifluction in the following three cases.

The first case involves the transition between the permafrost and seasonal frost zones. Permafrost newly produced by cooling may intensify seasonal frost heaving, where the formation of the impermeable layer improves moisture availability in the active layer. This possibly increases the rate of annual frost creep or gelifluction on thawing. Studies on the long-term advance of solifluction lobes often suggest variability in the rate of advance during the Holocene without substantial change in the thickness of moving soil mass (e.g., Benedict, 1970; Hirakawa, 1989). Part of such a variation may have accompanied the decay and growth of permafrost, although there are other possible sources of the variability, including change in snow condition, an episodic thaw event and even the low accuracy of the time markers (cf. Matthews et al., 1993). It should also be noted, however, that permafrost formation does not necessarily enhance moisture availability and thus solifluction rates, for instance, where a slope convexity allows free drainage over permafrost, or where permafrost occurs in the bedrock beneath the regolith.

The second case concerns the transition from the warm permafrost to cold permafrost zone. As the permafrost temperature lowers, two-sided freezing may replace one-sided freezing, where the whole active layer consists of fine-textured soil and poor drainage supports high moisture content of the active layer during summer. Two-sided freezing redistributes ice lenses near the bottom of the active layer. On thawing, plug-like flow may increase both D_M and V_{VL} (Woo et al., 1992). Where cooling of permafrost is not accompanied by the occurrence of two-sided freezing, however, no change may take place in solifluction processes.

Third, the maximum freeze–thaw depth varies irrespective of the presence of permafrost. This may also be responsible for change in the depth of ice lens formation and thus in both D_M and V_{VL}, where the fine soil is thick enough. In the seasonal frost zone, an increase in D_F would play a decisive role in activating solifluction lobes, as D_F approaches the potential D_M value. Moreover, an episodic warm summer in the permafrost zone may induce partial thawing of ice-rich permafrost, followed by temporary deepening and acceleration of soil movement. Some large solifluction lobes could have developed by such episodic events (cf. Benedict, 1970).

Another potential thermal influence is the impact of atmospheric warming on vegetation cover. Thus, a formerly bare ground surface may become vegetated, the vegetation influencing solifluction through its binding and thermal insulating effects. First, the vegetation mat would significantly decrease D_F in a seasonal frost environment. Simultaneously, a decrease in D_T may also occur in a permafrost environment, despite partially being offset by rising air temperatures in summer. Such a decline in the freeze–thaw depth may also reduce D_M and V_{VL}.

The second role of vegetation is to inhibit diurnal freeze–thaw action which, in its absence, occurs most frequently within the uppermost decimeter of soil. This effect would reduce solifluction on many high mountain slopes which experience potentially high freeze–thaw frequency and hold only thin regolith.

Long-term change in the amount of precipitation (snow or rain) affects the soil moisture regime. Snow has contrasting effects on solifluction. On one hand, it acts as a thermal insulator like vegetation. Late-lying snow patches inhibit diurnal freeze–thaw action in spring. Where a heavy snowfall covers the ground prior to winter, the autumn freeze–thaw activity or even the seasonal frost penetration is prevented or reduced (French, 1996, p. 67). This insulating effect generally reduces V_S. On the other hand, late-lying snow patches provide meltwater to the seasonally thawing ground, possibly increasing mobility of the soil mass and thus promoting gelifluction (Harris, 1972; Smith, 1988). In addition, meltwater maintains a high groundwater level until autumn at some sites, intensifying diurnal freeze–thaw action and increasing the amount of seasonal frost heave (Benedict, 1970); this possibly accelerates frost creep (both diurnal and annual) and gelifluction. Playing a similar role, rainfall in autumn also enhances solifluction (Matsuoka, 1996).

In summary, the prediction of the effect of climate change on solifluction requires understanding of the interaction between changes in air temperature, rainfall amount, distribution and duration of snow cover, type of freeze–thaw action, soil condition and vegetation.

8. Conclusions and prospects

Solifluction occurs widely from Antarctic nunataks to tropical mountains with large spatial variation in its nature. Solifluction involves several components: (1) needle ice creep and diurnal frost creep originating from diurnal freeze–thaw action; (2) annual frost creep, gelifluction and plug-like flow originating from annual freeze–thaw action; and (3) retrograde movement caused by soil cohesion. Long-term soil movement eventually leads to the development of features characterizing periglacial slopes, such as lobes, sheets, hummocks and stripes.

Processes and rates of solifluction and resulting landforms vary with climatic conditions, depending mainly on the depth and thickness of ice lense formation in the ground and the freeze–thaw frequency. Near the warm margin of the solifluction-affected environment, shallow but frequent diurnal frost induces relatively rapid movement of the superficial layer typically 5–10 cm thick; where needle ice creep prevails, the surface velocity can reach ~ 100 cm year^{-1}. This type of solifluction often develops thin stone-banked lobes (with a riser height < 30 cm) typically seen on tropical high mountains. The seasonal frost and warm permafrost regions, which encompass most of the mid-latitude high mountains and subpolar mountains, can experience seasonal freeze–thaw penetration to 50–200 cm and both diurnal and annual freeze–thaw cycles. In this zone, rapid but shallow soil movement (diurnal frost creep and needle ice creep) dominates high mountain slopes that hold only thin fine debris (< 20 cm) and lack vegetation, possibly producing thin lobes like in the tropical mountains. In contrast, where fine debris is thick, seasonal frost heaving followed by thaw consolidation induces annual frost creep or gelifluction of a soil mass up to a few decimeters thick, commonly at a rate of centimeters per year; this process may eventually yield medium-sized solifluction lobes with a riser height of 30–200 cm. In High-Arctic cold permafrost regions, two-sided freezing can induce plug-like flow of a soil mass 50–100 cm thick, while superficial movement driven by diurnal freeze–thaw action is lacking. Such deep movements may result in a thick lobe or sheet but also occur on slopes without any obvious solifluction landforms. The correlation between process and landform suggests that riser height can be used as an indicator of the maximum depth of soil movement and prevailing freeze–thaw action. Climate change may provide a different ground freezing (and vegetation) condition, which influences the surface velocity and maximum depth of movement.

Other factors controlling solifluction include soil moisture and topography. High water levels or frequent rainfalls in autumn to early winter enhance diurnal freeze–thaw action and subsequent seasonal frost heaving. Seasonal thawing of such an inten-

sively heaved layer, possibly aided by meltwater from a prolonged snow patch, can raise the moisture content of the thawed soil and promote gelifluction, or even produce rapid flows or slides. The slope angle defines the upper limit of the surface velocity of solifluction. The potential frost creep computed from the frost heave amount roughly approximates the observed surface velocity. A diagram correlating the two values permits an inter-site comparison of the relative magnitude of solifluction components.

One of the goals of the solifluction studies is to construct a predictive model of slope evolution in periglacial environments. Although attempts have been made to propose mathematical models of the rate of diurnal frost creep (Matsuoka, 1998b) or gelifluction (Kirkby, 1995; Lewkowicz and Clarke, 1998), modelling of landforms resulting from solifluction is still lacking. Ongoing studies suggest that, for instance, the evolution of a medium-sized solifluction lobe can be expressed as a function of such parameters as soil characteristics (thickness, grain size and consistency), inclination, moisture regime, freeze–thaw depth and number of annual freeze–thaw cycles. Physically based modelling of the lobe evolution requires (1) detailed field monitoring of these factors, (2) more accurate data on contemporary and long-term rates of the lobe advance and (3) laboratory analysis and simulation for exploring the influences of these factors on soil movement.

Acknowledgements

This study was financially supported by the Sumitomo Foundation and the Tokyo Geographical Society. I would like to thank Charles Harris and Antoni Lewkowicz for their comments that help improve the manuscript.

References

Åkerman, H.J., 1996. Slow mass movements and climatic relationships, 1972–1994, Kapp Linné, West Spitsbergen. In: Anderson, M.G., Brooks, S.M. (Eds.), Advances in Hillslope Processes, vol. 2. Wiley, Chichester, pp. 1219–1256.

Alexander, C.S., Price, L.W., 1980. Radiocarbon dating of the rate of movement of two solifluction lobes in the Ruby Range, Yukon Territory. Quat. Res. 13, 365–379.

Andersson, J.G., 1906. Solifluction, a component of subaerial denudation. J. Geol. 14, 91–112.

Auzet, A.-V., Ambroise, B., 1996. Soil creep dynamics, soil moisture and temperature conditions on a forested slope in the granitic Vosges Mountains, France. Earth Surf. Processes Landforms 21, 531–542.

Ballantyne, C.K., Harris, C., 1994. The Periglaciation of Great Britain. Cambridge Univ. Press, Cambridge.

Benedict, J.B., 1970. Downslope soil movement in a Colorado alpine region: rates, processes, and climatic significance. Arct. Alp. Res. 2, 165–226.

Benedict, J.B., 1976. Frost creep and gelifluction features: a review. Quat. Res. 6, 55–76.

Bennett, L.P., French, H.M., 1991. Solifluction and the role of permafrost creep, eastern Melville Island, N.W.T., Canada. Permafrost Periglac. Process. 2, 95–102.

Bertran, P., Francou, B., Texier, J.P., 1995. Stratified slope deposits: the stone-banked sheets and lobes model. In: Slaymaker, O. (Ed.), Steepland Geomorphology. Wiley, Chichester, pp. 147–169.

Boelhouwers, J.C., 1994. Periglacial landforms at Giant's Castle, Natal Drakensberg, South Africa. Permafrost Periglac. Process. 5, 129–136.

Boelhouwers, J.C., 1995. Present day soil frost activity at the Hexriver Mountains, western Cape, South Africa. Z. Geomorphol. N. F. 39, 237–248.

Caine, T.N., 1963. Movement of low angle scree slopes in the Lake District, northern England. Rev. Geomorphol. Dyn. 140, 171–177.

Douglas, T.D., Harrison, S., 1996. Turf-banked terraces in Öraefi, Southeast Iceland: morphometry, rates of movement, and environmental controls. Arct. Alp. Res. 28, 228–236.

Egginton, P.A., French, H.M., 1985. Solifluction and related processes, eastern Banks Island, N.W.T. Can. J. Earth Sci. 22, 1671–1678.

Fahey, B.D., 1974. Seasonal frost heave and frost penetration measurements in the Indian Peaks region of the Colorado Front Range. Arct. Alp. Res. 6, 63–70.

Francou, B., Bertran, P., 1997. A multivariate analysis of clast displacement rates on stone-banked sheets, Cordillera Real, Bolivia. Permafrost Periglac. Process. 8, 371–382.

French, H.M., 1996. The Periglacial Environment, 2nd ed. Longman, Essex.

French, H.M., Guglielmin, M., 1999. Observations on the ice-marginal, periglacial geomorphology of Terra Nova Bay, northern Victoria Land, Antarctica. Permafrost Periglac. Process. 10, 331–347.

Gamper, M.W., 1981. Heutige Solifluktionsbeträge von Erdströmen und klimamorphologische Interpretation fossiler Böden. Ergeb. Wiss. Unters. Schweiz. Nationalpark 79, 355–443.

Gamper, M.W., 1983. Controls and rates of movement of solifluction lobes in the eastern Swiss Alps. Proc. 4th Int. Conf. Permafrost (Fairbanks, Alaska). Natl. Acad. Sci., Washington, DC, pp. 433–438.

Gengnian, L., Heigang, X., Zhijiu, C., 1995. Gelifluction in the

alpine periglacial environment of the Tianshan Mountains, China. Permafrost Periglac. Process. 6, 265–271.
Gorbunov, A.P., Seversky, E.V., 1999. Solifluction in the mountains of Central Asia: distribution, morphology, processes. Permafrost Periglac. Process. 10, 81–89.
Graf, K., 1976. Zur Mechanik von Frostmusterungsprozessen in Boliviern und Ecuador. Z. Geomorphol. N. F. 20, 417–447.
Hall, K., 1983. Sorted stripes on sub-Antarctic Kerguelen Island. Earth Surf. Processes Landforms 8, 115–124.
Hansen-Bristow, K.J., Price, L.W., 1985. Turf-banked terraces in the Olympic Mountains, Washington, USA. Arct. Alp. Res. 17, 261–270.
Harris, C., 1972. Processes of soil movement in turf-banked solifluction lobes, Okistindan, northern Norway. In: Price, R.J., Sugden, D.E. (Eds.), Polar Geomorphology. Inst. Br. Geogr. Spec. Publ., vol. 4, pp. 155–174.
Harris, C., 1981. Periglacial Mass-Wasting: A Review of Research. BGRG Research Monograph, vol. 4, Geo Abstracts, Norwich.
Harris, C., 1989. Mechanisms of mass movement in periglacial environments. In: Anderson, M.G., Richards, K.S. (Eds.), Slope Stability. Wiley, Chichester, pp. 531–559.
Harris, C., Davies, M.C.R., 2000. Gelifluction: observations from large-scale laboratory simulations. Arct. Alp. Res. 32, 202–207.
Harris, C., Gallop, M., Coutard, J.-P., 1993. Physical modelling of gelifluction and frost creep: some results of a large-scale laboratory experiment. Earth Surf. Processes Landforms 18, 383–398.
Harris, C., Davies, M.C.R., Coutard, J.-P., 1997. Rates and processes of periglacial solifluction: an experimental approach. Earth Surf. Processes Landforms 22, 849–868.
Harris, S.A., Cheng, G., Zhao, X., Yongqin, D., 1998. Nature and dynamics of an active block stream, Kunlun Pass, Qinghai Province, People's Republic of China. Geogr. Ann. 80A, 123–133.
Hastenrath, S., 1973. Observations on the periglacial morphology of Mts. Kenya and Kilimanjaro, East Africa. Z. Geomorphol. N. F. 16, 161–179.
Higashi, A., Corte, A.E., 1971. Solifluction: a model experiment. Science 171, 480–482.
Hirakawa, K., 1989. Downslope movement of solifluction lobes in Iceland: a tephrostratigraphic approach. Geogr. Rep. Tokyo Metropolitan Univ. 24, 15–30.
Ishii, T., 1976. Slow movement of slope materials through the processes of freezing and thawing in the northern part of Ashio Mountains, Japan (in Japanese). Geogr. Rev. Jpn. 49, 523–537.
Jaesche, P., Veit, H., Stingl, H., Huwe, B., 1997. Influence of water and heat dynamics on solifluction movements in a periglacial environment in the Eastern Alps (Austria). In: Iskandar, I.K. (Ed.), Proc. Int. Symp., Physics, Chemistry and Ecology of Seasonally Frozen Soils (Fairbanks, Alaska), CRREL Spec. Rep. 97-10. pp. 80–86.
Jahn, A. et al., 1985. Experimental observations of periglacial processes in the Arctic. In: Church, M., Slaymaker, O. (Eds.), Field and Theory. Lectures in Geocryology, Univ. British Columbia Press, Vancouver, pp. 17–34.
Jahn, A., 1991. Slow soil movement in Tarfala Valley, Kebnekaise Mountains, Swedish Lapland. Geogr. Ann. 73A, 93–107.
Kirkby, M.J., 1995. A model for variations in gelifluction rates with temperature and topography: implications for global change. Geogr. Ann. 77A, 269–278.
Kranz, W.B., 1990. Self-organization manifest as patterned ground in recurrently frozen soils. Earth-Sci. Rev. 29, 117–130.
Lawler, D.M., 1986. River bank erosion and the influence of frost: a statistical examination. Trans. Inst. Br. Geogr. N.S. 11, 227–245.
Lawler, D.M., 1988. Environmental limits of needle ice: a global survey. Arct. Alp. Res. 20, 137–159.
Lewkowicz, A.G., 1988. Slope processes. In: Clark, M.J. (Ed.), Advances in Periglacial Geomorphology. Wiley, Chichester, pp. 325–368.
Lewkowicz, A.G., 1992a. Factors affecting the distribution and initiation of active-layer detachment slides on Ellesmere Island, Arctic Canada. In: Dixon, J.C., Abrahams, A.D. (Eds.), Periglacial Geomorphology. Wiley, Chichester, pp. 223–250.
Lewkowicz, A.G., 1992b. A solifluction meter for permafrost sites. Permafrost Periglac. Process. 3, 11–18.
Lewkowicz, A.G., Clarke, S., 1998. Late-summer solifluction and active layer depths, Fosheim Peninsula, Ellesmere Island, Canada. In: Lewkowicz, A.G., Allard, M. (Eds.), Proc. 6th Int. Conf. Permafrost (Yellowknife, Canada). Centre d'études nordiques. Univ. Laval, Sainte-Foy, pp. 641–666.
Mackay, J.R., 1981. Active layer slope movement in a continuous permafrost environment, Garry Island, Northwest Territories, Canada. Can. J. Earth Sci. 18, 1666–1680.
Mackay, J.R., Mathews, W.E., 1974. Movement of sorted stripes, the Cinder Cone, Garibaldi Park, BC, Canada. Arct. Alp. Res. 6, 347–359.
Maekado, A., Matsukura, Y., 1985. Recession of cutting slope made of loosely consolidated Quaternary deposits due to freeze–thaw action. Z. Geomorphol. N. F. 29, 213–222.
Mark, A.F., 1994. Patterned ground activity in a southern New Zealand high-alpine cushionfield. Arct. Alp. Res. 26, 270–280.
Matsuoka, N., 1994. Continuous recording of frost heave and creep on a Japanese alpine slope. Arct. Alp. Res. 26, 245–254.
Matsuoka, N., 1996. Soil moisture variability in relation to diurnal frost heaving on Japanese high mountain slopes. Permafrost Periglac. Process. 7, 139–151.
Matsuoka, N., 1998a. The relationship between frost heave and downslope soil movement: field measurements in the Japanese Alps. Permafrost Periglac. Process. 9, 121–133.
Matsuoka, N., 1998b. Modelling frost creep rates in an alpine environment. Permafrost Periglac. Process. 9, 397–409.
Matsuoka, N., Hirakawa, K., 2000. Solifluction resulting from one-sided and two-sided freezing: field data from Svalbard. Polar Geosci. 13, 187–201.
Matsuoka, N., Moriwaki, K., 1992. Frost heave and creep in the Sør Rondane Mountains, Antarctica. Arct. Alp. Res. 24, 271–280.

Matsuoka, N., Hirakawa, K., Watanabe, T., Moriwaki, K., 1997. Monitoring of periglacial slope processes in the Swiss Alps: the first two years of frost shattering, heave and creep. Permafrost Periglac. Process. 8, 155–177.

Matthews, J.A., Harris, C., Ballantyne, C.K., 1986. Studies on a gelifluction lobe, Jotunheimen, Norway: ^{14}C chronology, stratigraphy, sedimentology and palæoenvironment. Geogr. Ann. 68A, 345–360.

Matthews, J.A., Ballantyne, C.K., Harris, C., McCarroll, D., 1993. Solifluction and climatic variation in the Holocene: discussion and synthesis. In: Frenzel, B. (Ed.), Solifluction and Climatic Variation in the Holocene. Gustav Fisher Verlag, Stuttgart, pp. 339–361.

Nakaya, A., 1995. The effect of vegetation types on mass-movement caused by freezing and thawing (in Japanese). Univ. Tsukuba, Master Thesis.

Nesje, A., Knamme, M., Rye, N., 1989. Neoglacial gelifluction in the Jostedalsbreen region, western Norway: evidence from dated buried palaeopodsols. Earth Surf. Processes Landforms 14, 259–270.

Noguchi, Y., Tabuchi, H., Hasegawa, H., 1987. Physical factors controlling the formation of patterned ground on Haleakala, Maui. Geogr. Ann. 69A, 329–342.

Nyberg, R., 1993. Freeze–thaw activity and some of its geomorphic implications in the Abisko Mountains, Swedish Lappland. Permafrost Periglac. Process. 4, 37–47.

Pérez, F.L., 1987. Downslope stone transport by needle ice in a High Andean area (Venezuela). Rev. Geomorphol. Dyn. 36, 33–51.

Pérez, F.L., 1988. The movement of debris on a high Andean talus. Z. Geomorphol. N. F. 32, 77–99.

Pérez, F.L., 1992. Miniature sorted stripes in the Páramode Piedras Blancas (Venezuelan Andes). In: Dixon, J.C., Abrahams, A.D. (Eds.), Periglacial Geomorphology. Wiley, Chichester, pp. 125–157.

Pissart, A., 1993. Understanding the controls on solifluction movements in different environments: a methodology and its application in the French Alps. In: Frenzel, B. (Ed.), Solifluction and Climatic Variation in the Holocene. Gustav Fisher Verlag, Stuttgart, pp. 209–215.

Price, L.W., 1973. Rates of mass wasting in the Ruby Range, Yukon Territory. Permafrost, 2nd Int. Conf. (Yakutsk, USSR), North Amer. Contribution. Natl. Acad. Sci., Washington, DC, pp. 235–245.

Price, L.W., 1991. Subsurface movement on solifluction slopes in the Ruby Range, Yukon Territory, Canada: a 20-year study. Arct. Alp. Res. 23, 200–205.

Rapp, A., 1960. Recent development of mountain slopes in Kärkevagge and surroundings, Northern Scandinavia. Geogr. Ann. 42A, 65–200.

Rapp, A., Åkerman, H.J., 1993. Slope processes and climate in the Abisko Mountains, northern Sweden. In: Frenzel, B. (Ed.), Solifluction and Climatic Variation in the Holocene. Gustav Fisher Verlag, Stuttgart, pp. 163–177.

Reanier, R.E., Ugolini, F.C., 1983. Gelifluction deposits as sources of paleoenvironmental information. Proc. 4th Int. Conf. Permafrost (Fairbanks, Alaska). Natl. Acad. Press, Washington, DC, pp. 1042–1047.

Repelewska-Pękalowa, J., Pękala, K., 1993. The influence of local factors on solifluction rates, Spitsbergen, Svalbard. In: Frenzel, B. (Ed.), Solifluction and Climatic Variation in the Holocene. Gustav Fisher Verlag, Stuttgart, pp. 251–266.

Rudberg, S., 1962. A report on some field observations concerning periglacial geomorphology and mass movement on slopes in Sweden. Biul. Peryglacjalny 11, 311–323.

Sawaguchi, S., 1995. Rates and processes of mass movement on periglacial rubble slopes in Spitsbergen (in Japanese). J. Geogr. 104, 874–894.

Sawaguchi, S., Koaze, T., 1998. Field experiment on periglacial mass movement and frost heave in the Kitakami Mountains, northeastern Japan (in Japanese). Trans. Jpn. Geomorphol. Union 19, 221–242.

Selkirk, J.M., 1998. Active vegetation-banked terraces on Macquarie Island. Z. Geomorphol. N. F. 42, 483–496.

Smith, J., 1960. Cryoturbation data from South Georgia. Biul. Peryglacjalny 8, 73–79.

Smith, D.J., 1987a. Frost-heave activity in the Mount Rae area, Canadian Rocky Mountains. Arct. Alp. Res. 19, 155–166.

Smith, D.J., 1987b. Late Holocene solifluction lobe activity in the Mount Rae area, southern Canadian Rocky Mountains. Can. J. Earth Sci. 24, 1634–1642.

Smith, D.J., 1988. Rates and controls of soil movement on a solifluction slope in the Mount Rae area, Canadian Rocky Mountains. Z. Geomorphol. N. F. Suppl. 71, 25–44.

Smith, D.J., 1992. Long-term rates of contemporary solifluction in the Canadian Rocky Mountains. In: Dixon, J.C., Abrahams, A.D. (Eds.), Periglacial Geomorphology. Wiley, Chichester, pp. 203–221.

Sohma, H., Okazawa, S., Iwata, S., 1979. Slow mass-movement processes in an alpine region of Mt. Shirouma Dake, the Japan Alps (in Japanese). Geogr. Rev. Jpn. 52, 562–579.

Sone, T., Shiraiwa, T., Kitahara, T., 1998. Surface stone movements on stone-banked lobes in a nivation hollow on the Daisetsu Mountains, Hokkaido, Japan (in Japanese). Quat. J. Geogr. 50, 201–207.

Washburn, A.L., 1967. Instrumental observations of mass-wasting in the Mesters Vig district, Northeast Greenland. Medd. Groenl. 166, 318 pp.

Washburn, A.L., 1979. Geocryology: A Survey of Periglacial Processes and Environments. Edward Arnold, London.

Washburn, A.L., 1999. A High Arctic frost-creep/gelifluction slope, 1981–89: Resolute Bay, Cornwallis Island, Northwest Territories, Canada. Permafrost Periglac. Process. 10, 163–186.

Williams, P.J., 1966. Downslope soil movement at a sub-Arctic location with regard to variations with depth. Can. Geotech. J. 3, 191–203.

Williams, P.J., Smith, M.W., 1989. The Frozen Earth: Fundamentals of Geocryology. Cambridge Univ. Press, Cambridge.

Woo, M., Lewkowicz, A.G., Rouse, W.R., 1992. Response of the Canadian permafrost environment to climate change. Phys. Geogr. 13, 287–317.

Worsley, P., 1993. Holocene solifluction at Okstindan, northern

Norway: a reassessment. In: Frenzel, B. (Ed.), Solifluction and Climatic Variation in the Holocene. Gustav Fisher Verlag, Stuttgart, pp. 49–57.

Yamada, S., 1997. Seasonal variation in soil creep on a forested hillslope near Sapporo, Hokkaido, northern Japan. Trans. Jpn. Geomorphol. Union 18, 117–130.

Yamada, S., Matsumoto, H., Hirakawa, K., 2000. Seasonal variation in creep and temperature in a solifluction lobe: continuous monitoring in the Daisetsu Mountains, northern Japan. Permafrost Periglac. Process. 11, 125–135.

Zhu, C., 1996. Rates of periglacial processes in the central Tianshan, China. Permafrost Periglac. Process. 7, 79–84.